The Cryosphere, 18, 5735–5752, 2024
https://doi.org/10.5194/tc-18-5735-2024
© Author(s) 2024. This work is distributed under
the Creative Commons Attribution 4.0 License.

The Cryosphere Open Access EGU

# The macronutrient and micronutrient (iron and manganese) content of icebergs

**Jana Krause[1], Dustin Carroll[2], Juan Höfer[3,4], Jeremy Donaire[5,6], Eric P. Achterberg[1], Emilio Alarcón[4], Te Liu[1], Lorenz Meire[7,8], Kechen Zhu[9], and Mark J. Hopwood[9]**

[1]GEOMAR Helmholtz Centre for Ocean Research Kiel, Kiel, Germany
[2]Moss Landing Marine Laboratories, San José State University, Moss Landing, California, USA
[3]Escuela de Ciencias del Mar, Pontificia Universidad Católica de Valparaíso, Valparaíso, Chile
[4]Centro FONDAP de Investigación en Dinámica de Ecosistemas Marinos de Altas Latitudes (IDEAL), Valdivia, Chile
[5]Facultad de Ingeniería, Universidad Andrés Bello, Viña del Mar, Chile
[6]Faculty of Sciences and Bioengineering Sciences, Vrije Universiteit Brussel, Brussels, Belgium
[7]Department of Estuarine & Delta Systems, Royal Netherlands Institute for Sea Research, Yerseke, the Netherlands
[8]Greenland Climate Research Centre, Greenland Institute of Natural Resources, Nuuk, Greenland
[9]Department of Ocean Science and Engineering, Southern University of Science and Technology, Shenzhen, China

**Correspondence:** Mark J. Hopwood (mark@sustech.edu.cn)

Received: 12 December 2023 – Discussion started: 9 January 2024
Revised: 17 October 2024 – Accepted: 18 October 2024 – Published: 10 December 2024

**Abstract.** Ice calved from the Antarctic and Greenland ice sheets or tidewater glaciers ultimately melts in the ocean, contributing to sea-level rise and potentially affecting marine biogeochemistry. Icebergs have been described as ocean micronutrient fertilizing agents and biological hotspots due to their potential roles as platforms for marine mammals and birds. Icebergs may be especially important fertilizing agents in the Southern Ocean, where low availability of the micronutrients iron and manganese extensively limits marine primary production. Whilst icebergs have long been described as a source of iron to the ocean, their nutrient load is poorly constrained and it is unclear if there are regional differences. Here we show that 589 ice fragments collected from calved ice in contrasting regions spanning the Antarctic Peninsula; Greenland; and smaller tidewater systems in Svalbard, Patagonia, and Iceland have similar (micro)nutrient concentrations with limited or no significant differences between regions. Icebergs are a minor or negligible source of macronutrients to the ocean with low concentrations of $NO_x^-$ ($NO_3^- + NO_2^-$; median of 0.51 µM), $PO_4^{3-}$ (median of 0.04 µM), and dissolved Si (dSi; median of 0.02 µM). In contrast, icebergs deliver elevated concentrations of dissolved Fe (dFe; median of 12 nM) and Mn (dMn; median of 2.6 nM). The sediment load for Antarctic ice (median of 9 mg $L^{-1}$, $n = 144$) was low compared to prior reported values for the Arctic (up to 200 g $L^{-1}$). Total dissolvable Fe and Mn retained a strong relationship with the sediment load (both $R^2 = 0.43$, $p < 0.001$), whereas weaker relationships were observed for dFe ($R^2 = 0.30$, $p < 0.001$), dMn ($R^2 = 0.20$, $p < 0.001$), and dSi ($R^2 = 0.29$, $p < 0.001$). A strong correlation between total dissolvable Fe and Mn ($R^2 = 0.95$, $p < 0.001$) and a total dissolvable Mn : Fe ratio of 0.024 suggested a lithogenic origin for the majority of sediment present in ice. Dissolved Mn was present at higher dMn : dFe ratios, with fluxes from melting ice roughly equivalent to 30 % of the corresponding dFe flux. Our results suggest that $NO_x^-$ and $PO_4^{3-}$ concentrations measured in calved icebergs originate from the ice matrix. Conversely, high Fe and Mn, as well as occasionally high dSi concentrations, are associated with englacial sediment, which experiences limited biogeochemical processing prior to release into the ocean.

## 1 Introduction

At the interface between marine-terminating ice and the ocean, icebergs are physical and chemical agents via which ice–ocean interactions affect marine biogeochemical cycles

(Enderlin et al., 2016; Helly et al., 2011; Smith et al., 2007). Icebergs are widely characterized as a source of the micronutrient iron (Fe) to marine ecosystems (Raiswell, 2011; Raiswell et al., 2008; Shaw et al., 2011), especially in the Southern Ocean (Schwarz and Schodlok, 2009; Smith et al., 2007; Vernet et al., 2011). Iron availability is a major factor limiting primary production in the Southern Ocean (Martin et al., 1990a, b; Moore et al., 2013), and thus regional changes in the Fe supply can have pronounced ecosystem effects (Schwarz and Schodlok, 2009; Wu and Hou, 2017). Whilst icebergs are recognized as a potentially climatically sensitive Fe source (IPCC, 2019), the importance of their role in the delivery of other micro- and macronutrients remains to be quantified. Recent work has, for example, suggested that low dissolved manganese (Mn) concentrations are a further co-limiting factor for phytoplankton growth in parts of the Southern Ocean (Browning et al., 2021; Hawco et al., 2022; Latour et al., 2021). As Fe and Mn share similar sources, icebergs might also be an equally important source term for the polar marine Mn cycle (Forsch et al., 2021).

In contrast to Antarctica, Fe limitation of marine phytoplankton growth in the Arctic is a less prominent feature largely confined to offshore areas of the high-latitude North Atlantic away from typical iceberg trajectories (Nielsdottir et al., 2009; Ryan-Keogh et al., 2013). Phytoplankton growth within regions around Greenland affected by icebergs is more often limited by nitrate availability (Randelhoff et al., 2020; Krisch et al., 2020). With icebergs thought to supply only limited concentrations of nitrate and phosphate to the ocean, a direct iceberg fertilization effect is not expected in nitrate-limited marine regions (Shulenberger, 1983). However, icebergs could be a modest source of silica to the marine environment (Hawkings et al., 2017; Meire et al., 2016), which might have ecological effects. Dissolved silica (dSi) availability often limits diatom growth in the Arctic due to its depletion prior to nitrate (Krause et al., 2018, 2019).

In order to understand how iceberg-derived fluxes of (micro)nutrients may change regionally with climate change and glacier retreat inland, it is necessary to understand the origin and fate of nutrients within calved icebergs at sea. The nutrient load of icebergs can be broadly separated into processes which affect the nutrient concentration of the ice matrix (Fischer et al., 2015; Hansson, 1994) and processes associated with sediment incorporation (Alley et al., 1997; Knight, 1997; Mugford and Dowdeswell, 2010). Internal cycling may also critically re-distribute (micro)nutrients and affect the relative abundance of elements in both dissolved ($< 0.2\,\mu m$) and particulate ($> 0.2\,\mu m$) phases. Some fraction of the labile phases in englacial sediments – particularly for the elements Fe, Mn, and silica, which are present at high abundances – may ultimately be transformed into bioaccessible nutrients in the ocean (Forsch et al., 2021; Hawkings et al., 2017; Raiswell, 2011). How sediment is gained and lost from ice before, during, and after iceberg calving might therefore exert some influence on measured (micro)nutrient concentrations in melting icebergs at sea (Hopwood et al., 2019).

On exposed ice surfaces during the growth season, cryoconite formation and the growth of algae are notable features which will act to re-distribute nutrients between inorganic and organic pools and to amplify heterogeneity in the distribution of nutrients within ice (Cook et al., 2015; Rozwalak et al., 2022; Stibal et al., 2017). These processes occur alongside and likely interact with other photochemical reactions (Kim et al., 2010, 2024). Whilst iceberg calving may temporarily disturb features present on ice surfaces and the rolling of smaller icebergs will regularly interrupt cryoconite growth on calved ice surfaces, long-lived icebergs may continue to accumulate the effects of photochemical processes and re-develop cryoconite. The nutrient content of icebergs, nutrient distributions, and their ratios might therefore not be static and in fact subject to semi-continuous changes.

As ice moves downstream from ice sheets to the coastline, critical physical processes may exert a strong influence on the characteristics of the ice which ultimately calves into the ocean (Smith et al., 2019). At the base of floating ice tongues and ice shelves, the melt rates of basal ice layers exposed to warm ocean waters can be rapid. Beneath the floating ice tongue of Nioghalvfjerdsbræ in northeastern Greenland, for example, a melt rate of $8.6 \pm 1.4\,m\,yr^{-1}$ is likely sufficient to remove most sediment-rich basal ice prior to iceberg calving (Huhn et al., 2021). In other similar cases worldwide, calved ice may ultimately be deprived of basal layers which might otherwise have carried distinct labile sediment loadings, reflecting subglacial processes (Smith et al., 2019). Nevertheless, following calving the nutrient content of ice may still be strongly affected by "new" ice–sediment interactions. Icebergs which become grounded or scour shallow coastal sediments may temporarily re-acquire a basal layer loaded with sediment (Gutt et al., 1996; Syvitski et al., 1987; Woodworth-Lynas et al., 1991). Scoured sediments may be physically and chemically distinct from those acquired from landslides or basal glacial processes and thus also temporarily introduce different nutrient ratios and concentrations into ice and meltwater (Forsch et al., 2021).

Finally, whilst many research questions concerning the effects of the cryosphere on the ocean relate to melting processes, marine ice formation is a mechanism via which ice growth can occur in the water column (Craven et al., 2009; Lewis and Perkin, 1986; Oerter et al., 1992). Marine ice is formed from supercooled seawater around Antarctica via the formation of platelet, or frazil, ice crystals. Whilst the chemical composition of this ice is poorly studied, measurements from the Amery Ice Shelf suggest marine ice has relatively high dissolved Fe (dFe) concentrations (e.g. 339–691 nM dFe, Herraiz-Borreguero et al., 2016). The origin of this dFe may be subglacial, potentially indicating a synergistic effect between subglacial and ice melt Fe sources. Similar synergistic effects have been suggested from model studies concern-

ing sea ice and ice shelves, whereby sea ice may trap and later release Fe that originates from ice shelves (Person et al., 2021). A "source-to-sink" narrative concerning iceberg-derived (micro)nutrient delivery from ice directly into the ocean may therefore be over-simplistic. It is important to recognize that the extent of spatial and temporal overlap between different (micro)nutrient sources may result in interactive effects in annual budgets. Such effects could arise due to the underlying physical processes and/or the seasonal timing of micro(nutrient) sources and sinks (Boyd et al., 2012; Person et al., 2021).

In order to evaluate whether or not there are regional differences in the (micro)nutrient content of icebergs and the associated fluxes into the ocean, here we assess the concentration of macronutrients ($NO_x^-$, dSi, and $PO_4^{3-}$), micronutrients (dissolved Fe and Mn), and total dissolvable metals (Fe and Mn) from calved ice across multiple Arctic and Antarctic catchments. In order to investigate potential spatial and temporal biases associated with seasonal shifts and the general targeting of smaller ice fragments to collect samples, we include repeat samples from five campaigns in Nuup Kangerlua (a fjord hosting three marine-terminating glaciers in southwestern Greenland) and a comparison of recently calved ice from inshore and offshore ice samples in Disko Bay (western Greenland). Throughout, we test the null hypothesis that icebergs from different regions have no differences in macronutrient or micronutrient (Fe and Mn) concentrations.

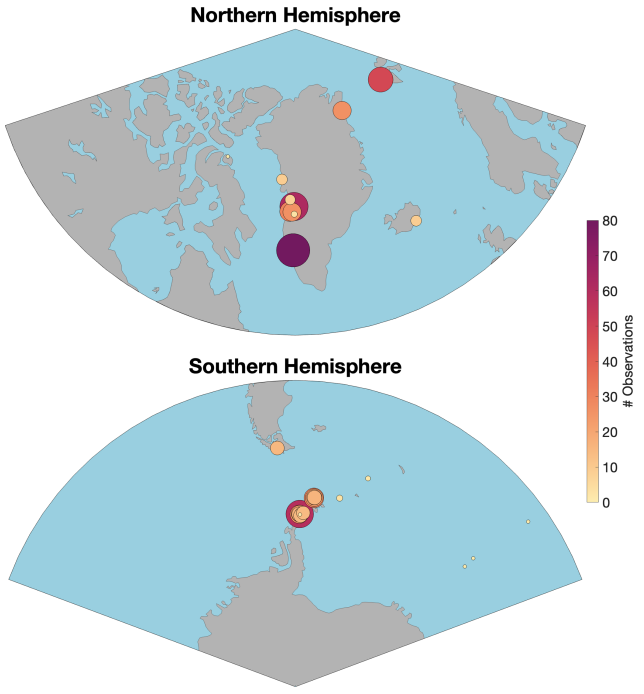


**Figure 1.** Sample distributions in the Northern Hemisphere and Southern Hemisphere. Literature values from prior work are included (see Table S1 for a full list of details).

## 2 Methods

### 2.1 Sample collection

Iceberg samples were collected by hand or using nylon nets to snag floating ice fragments. Sample collection was randomized at each field site location (Fig. 1 and Table S1 in the Supplement) by collecting ice samples at regular intervals along pre-defined transects; 1–5 kg ice pieces were retained in low-density polyethylene (LDPE) bags and melted at room temperature. The first three aliquots of meltwater were discarded to rinse the LDPE bags. Meltwater was then syringe-filtered (0.2 µm, polyvinyl difluoride, Millipore) into pre-cleaned 125 mL LDPE bottles for dissolved trace metal analysis and 20 mL polypropylene tubes for dissolved nutrient analysis. All plasticware for trace metal sample collection was pre-cleaned using a three-stage protocol: detergent, 1-week soak in HCl (1 M reagent grade), and 1-week soak in $HNO_3$ (1 M reagent grade) with three deionized water rinses after each stage. Filters for trace metal analysis were pre-rinsed with HCl (1 M reagent grade), followed by deionized water. Some unfiltered samples were also retained for total dissolvable metal analysis.

In Disko Bay (western Greenland), a targeted exercise was conducted to test whether distinct regional patterns of ice nutrient concentrations could be associated with specific calving locations. During the GLICE (Greenland's Icebergs and their biogeochemical impacts) cruise (R/V *Sanna*, August 2022) ice collection was conducted as per other regions close to the outflow of Sermeq Kujalleq (also known as Jakobshavn Isbræ) and Eqip Sermia (Table S1). Additionally, ice fragments were collected from two large icebergs in Disko Bay, referred to herein as fragments from the "Beluga" iceberg and "Narwhal" iceberg. These icebergs were tracked using the ship's radar by logging the coordinates and relative bearing of the approximate centre of the iceberg at regular time intervals. In Nuup Kangerlua (southwestern Greenland), samples were collected during five repeated campaigns spanning boreal spring and summer in different years (May 2014, July 2015, August 2018, May 2019, and September 2019) to assess the reproducibility of data from the same region by different teams deploying the same methods in different months and years.

### 2.2 Sediment load measurements

Wet sediment sub-samples were dried at 60 °C to determine sediment load (dry weight of sediment per unit volume, $mg\,L^{-1}$). The sediment load was determined for a subset of randomly collected ice samples in parallel with (micro)nutrients in the Antarctic Peninsula. In Maxwell Bay (King George Island), a targeted exercise was conducted to collect ice with embedded sediment. Eight large ice frag-

ments (10–45 kg) with sediment layers embedded within the ice were retained in sealed opaque plastic boxes. These fragments were specifically selected to avoid the possibility of including samples with surface sediment acquired by ice scouring the coastline or shallow sediments. Boxes were half-filled with seawater from the bay. Sediment-rich ice was left to melt in the dark with an air temperature of $\sim$ 5–10 °C. Periodically (after 2, 4, 8, 16, 24, and 48 h) the water was weighed and settled sediment was removed by decanting and filtration before estimating its dry weight.

### 2.3 Chemical measurements

Dissolved trace metal samples were acidified after filtration to pH 1.9 by addition of 180 µL HCl (UpA, ROMIL) and placed upright for > 6 months prior to analysis. Unfiltered trace metal samples were acidified similarly, and trace metals in these samples are subsequently referred to as "total dissolvable", which is defined as dissolved metals plus any additional metals present which are soluble at pH 1.9 after 6 months of storage. Analysis via inductively coupled plasma mass spectrometry (ICP-MS, Element XR, Thermo Fisher Scientific) was undertaken after dilution with indium-spiked 1 M $HNO_3$ (distilled in house from SPA grade $HNO_3$, Roth); 4 mL aliquots of total dissolvable samples were filtered (0.2 µm, polyvinyl difluoride, Millipore) immediately prior to analysis.

Calibration for Fe and Mn was via standard addition with a linear peak response from 1–1000 nM ($R^2 > 0.99$). Analysis of the reference material CASS-6 yielded a Fe concentration of $26.6 \pm 1.2$ nM (certified $27.9 \pm 2.1$ nM) and a Mn concentration of $37.1 \pm 0.83$ nM (certified $40.4 \pm 2.18$ nM). Due to the very broad range of Fe concentrations in ice samples, samples were run using varying dilution factors. Precision is improved at low dilution factors, so we report results from the lowest dilution factor that could be used to keep Fe and Mn concentrations within the calibrated range (in many cases dissolved samples could be run without dilution). Dissolved samples were initially run at a 10-fold dilution, using 1 M $HNO_3$. A 1 M $HNO_3$ blank from the same acid batch was analysed every 10 samples and in triplicate at the start and end of each sample rack (90 × 4 mL sample vials). Total dissolvable samples (unfiltered, acidified samples) were initially run at a 100-fold dilution followed by a 10-fold dilution for samples with nanomolar concentrations. Samples with measured concentrations of Fe or Mn < 25 nM were then re-run without dilution. Detection limits, assessed as 3 standard deviations of blank (1 M $HNO_3$) measurements, varied between batches (and dilution factors) but were invariably < 0.86 nM dFe and < 0.83 nM dMn (dissolved Mn) for the standard 10-fold dilution analyses. The field blank (deionized water filtered and processed as a sample) was below the detection limit. As in a majority of cases samples were run by dilution; the 1 M $HNO_3$ acid used to both dilute samples and run as a reagent blank every 10 samples was therefore considered the most useful blank measurement. Mean (± standard deviation) blank (1 M $HNO_3$) measurements varied by acid batch from $0.06 \pm 0.02$ nM dFe and $0.03 \pm 0.02$ nM dMn to $0.38 \pm 0.08$ nM dFe and $0.14 \pm 0.08$ nM dMn.

Where macronutrient samples were not collected in parallel with trace metals, samples preserved for trace metals were analysed for $PO_4^{3-}$ and dSi (this was not possible for $NO_x^-$ because of residual contamination from concentrated $HNO_3$ in LDPE bottles). Analysis of macronutrients was conducted for $NO_3^-$, $NO_2^-$, $PO_4^{3-}$, and dSi by segmented flow injection analysis using a QuAAtro (SEAL Analytical) autoanalyser (Hansen and Koroleff, 1999). Recoveries of a certified reference solution (KANSO, Japan) were 98 % ± 1 % $NO_x^-$, 99 % ± 1 % $PO_4^{3-}$, and 97 % ± 3 % dSi. Detection limits varied between sample batches and were < 0.10 µM $NO_x^-$, < 0.02 µM $NO_2^-$, < 0.10 µM $PO_4^{3-}$, and < 0.25 µM dSi.

### 2.4 Data compilation

In addition to new data from 367 new samples collected and analysed herein, existing comparable data were compiled from prior literature, most of which were processed in prior work by the same protocol in the same laboratories as those herein (see Table S1). Including prior work, a total of 589 samples are available for interpretation (note that not all samples were analysed for all parameters, so $n$ varies between statistical analyses). Previously published data include samples from Greenland, Svalbard, the Antarctic Peninsula, Patagonia, and Iceland (De Baar et al., 1995; Campbell and Yeats, 1982; Forsch et al., 2021; Höfer et al., 2019; Hopwood et al., 2017, 2019; Lin et al., 2011; Loscher et al., 1997; Martin et al., 1990b). Altogether, 575 out of the 589 samples reported were collected and analysed as described herein at the same laboratories. Only 14 literature values were from other laboratories, so there is a high degree of internal consistency in the methods used. Throughout concentrations are reported in units of $L^{-1}$, referring to the concentration measured in meltwater.

### 2.5 Statistical analysis

To test if icebergs had statistically significant regional differences in (micro)nutrient concentrations depending on their origin at a hemisphere, regional, or catchment scale, a multivariate PERMANOVA (permutational multivariate analysis of variance) was realized (function adonis2 from the vegan package, Oksanen et al., 2020) using the concentrations of trace metals (both dissolved and total dissolvable) and macronutrients ($NO_x^-$, $PO_4^{3-}$, and dSi). Along with this analysis non-metric multidimensional scaling (nMDS; function metaMDS from the vegan package, Oksanen et al., 2020) was used to compute the ordination of the iceberg samples depending on their nutrient concentrations. nMDS is an unconstrained ordination analysis that assesses the sim-

ilarities and dissimilarities among data points only using the set of variables informing the ordination (herein macro- and micronutrients concentrations). The variables considered for the analysis are summarized in orthogonal dimensions showing the more similar data points as closer (groupings of data points with similar characteristics) within the space created by the orthogonal dimensions. The same analyses were used to assess differences in Disko Bay samples collected in August 2022, in this case comparing iceberg samples collected in inshore ($< 1$ km from the coastline) and offshore ($> 15$ km from the coastline) zones. In both cases subsequent ANOVA (aov function from the stats package) and a Tukey test (TukeyHSD function from the stats package) were undertaken to test for significant differences in specific (micro)nutrient concentrations.

The relationship between iceberg sediment load and the concentration of trace metals (both dissolved and total dissolvable) and macronutrients was determined by means of a linear regression (lm function from the stats package). For this analysis two outliers were removed from the dataset because their sediment load values were over an order of magnitude larger (50 726 mg $L^{-1}$ and 6128 mg $L^{-1}$) than other values (total $n = 144$); including these two data points would have disproportionately skewed the relationships. Finally, to analyse how melting and sediment release rates changed over time using the incubations in Maxwell Bay, we used the same procedure as Höfer et al. (2018). In short, we first tested if the relationship between melting and sediment release rates and time better fitted a linear or exponential relationship using a second-order logistic regression. Then, we tested the fit of the selected relationship (exponential in this case) to see if the relationship was significant and determined the percentage of variance explained (lm function from the stats package). Since the initial conditions of each incubation (i.e. iceberg size, shape, and initial sediment load) varied, the rates for each individual experiment were normalized by dividing each rate by the maximum rate registered in the same incubation. All statistical analyses and figures (ggplot2 package) were realized using R version 4.3.2 (R Core Team, 2023).

## 3 Results

### 3.1 Nutrient distributions in the global iceberg dataset

A total of 589 ice fragments have been analysed to date. The combined data are more balanced compared to prior work in terms of the coverage of Antarctica (45 % of samples), Greenland (42 % of samples), and Svalbard (8.1 % of samples) and smaller sub-polar catchments in Patagonia, Canada, and Iceland (4.2 % of samples). There are however still some spatial biases in the data. Notably samples from Greenland are largely from the west (Fig. 1), and samples from Antarctica are all from the Antarctic Peninsula or downstream waters along the "Iceberg Alley" in the Weddell Sea and the South Atlantic sector of the Southern Ocean (Tournadre et al., 2016). Almost all samples were collected in summer, with only a subset of samples (from Nuup Kangerlua, Table S4 in the Supplement) collected in spring and autumn to investigate potential seasonal changes. At the catchment scale, Nuup Kangerlua (southwestern Greenland, also known as Godthåbsfjord, 15 % of the dataset), Eqip Sermia (western Greenland, 11 % of the dataset), Thunder Bay (western Antarctic Peninsula, 10 % of the dataset), Kongsfjorden (Svalbard, 8.2 % of the dataset), Disko Bay (western Greenland, 5.1 % of the dataset), and Nelson Island (northern Antarctic Peninsula, 5.1 % of the dataset) are particularly well represented. The other 23 catchments each account for $< 5$ % of the samples.

Average macronutrient concentrations in ice samples were low with median concentrations of 0.04 µM $PO_4^{3-}$, 0.54 µM $NO_3^-$, and 0.02 µM dSi. Throughout the dataset $NO_2^-$ was close to or below the limit of detection; thus $NO_3^-$ and $NO_x^-$ concentrations were practically identical, with $NO_2^-$ almost invariably constituting $< 10$ % of $NO_x^-$ (mean of 1.8 %). Mean nutrient concentrations in all cases were higher than median concentrations, and the large relative standard deviations indicated that variability between samples might mask any regional differences. Preliminary analysis revealed a large fraction of data below the limit of detection (i.e. concentrations $<$ LOD) for several components, particularly $PO_4^{3-}$ (24 % of all measurements $<$ LOD) and dSi (48 % of all measurements $<$ LOD). Other (micro)nutrients were less affected by detection limits; e.g. only 8 % of $NO_x^-$ concentrations were $<$ LOD. In any dataset with a large fraction of data $<$ LOD, how these values are treated makes some difference to calculated statistics, so reported averages vary for $PO_4^{3-}$ and dSi depending on how LOD values are treated. Removing values $<$ LOD entirely would skew the statistical analyses. For example, the median values reported above increase from 0.04 to 0.05 µM $PO_4^{3-}$ and 0.02 to 0.19 µM dSi if values $<$ LOD are excluded. For consistency throughout all statistical analyses, a value of "0" was therefore used to represent LOD data.

It has been previously reported that both total dissolvable Fe (TdFe) and dFe concentrations are extremely variable within ice samples collected at the same location (Hopwood et al., 2017; Lin and Twining, 2012; Lin et al., 2011). This remained the case with the expanded dataset herein with notable differences between the mean (82 nM dFe, 13 µM TdFe) and median concentrations (12 nM dFe, 220 nM TdFe) on a global scale. An extremely broad range of concentrations were also observed for both dissolved Mn (mean of 26 nM, median of 2.6 nM) and total dissolvable Mn (TdMn; mean of 150 nM, median of 10 nM). As for Fe, this reflected the skewed distribution of the dataset towards a small number of samples with extremely high concentrations. The highest 2 % of TdMn samples accounted for 79 % of the cumulative TdMn measured. Similarly, the highest 2 % of TdFe samples accounted for 77 % of the cumula-

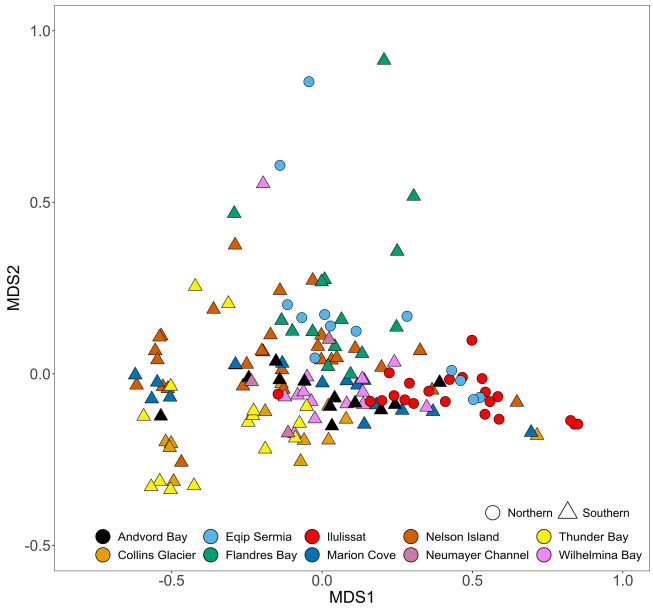


**Figure 2.** A scatter plot showing the results of an nMDS ordination analysis using macro- and micronutrient concentrations. Only samples with complete data for the following parameters are shown: $NO_x^-$, $PO_4^{3-}$, dSi, dFe, TdFe, dMn, and TdMn. A non-metric multidimensional scaling (nMDS) ordination is used to represent multi-dimensional data in a reduced number of dimensions. MDS1 and MDS2 are multidimensional scaling factors which represent the dissimilarities between the data sorted to catchment level. Data points represent individual samples. Data points which appear further apart are more different, whereas those that cluster together are more similar. A PERMANOVA analysis of iceberg nutrient concentrations showed significant differences at the catchment level ($R^2 = 0.24$, $p$ value $< 0.001$). Shapes denote the hemispheres, while colours denote specific sampling locations.

tive TdFe measured. Accordingly, there were very high relative standard deviations for both mean dMn ($26 \pm 160$ nM) and TdMn ($150 \pm 1500$ nM) which, as for Fe, remained high when data were grouped by region or catchment. Considering all (micro)nutrients measured, there were no significant differences in the iceberg chemical composition at a hemispheric ($p$ value $= 0.16$) or regional ($p$ value $= 0.16$) level. However, a PERMANOVA analysis showed significant differences ($R^2 = 0.24$, $p$ value $< 0.001$) at a catchment level. Similarly, an nMDS analysis (stress $= 0.07$) showed that samples from the same catchment tended to be grouped closer together (Fig. 2) and in general Antarctic samples were distributed on the left side, whereas Arctic samples were more abundant on the right side of the ordination analysis (Fig. 2).

The ratio of TdFe : TdMn was linear ($R^2 = 0.95$, calculated excluding the highest 2 % of Mn and Fe concentrations to avoid skewing the gradient, Fig. 3). Furthermore, the total dissolvable Mn : Fe ratio of 0.023 (linear regression of TdMn $= 0.023 \times$ [TdFe]) was close to mean continental-crust composition, which is approximately 0.1 % MnO and 5.04 % FeO by weight (producing a ratio of 0.020) (Rudnick and Gao, 2004). In contrast, no clear relationship was observed between dFe and dMn. For all data, all Antarctic data, and all Greenlandic data, respectively, the mean dMn : dFe (0.47, 0.50, and 0.28) and median dMn : dFe (0.17, 0.19, and 0.11) ratios were however consistently higher than the TdMn : TdFe ratio. This indicates an excess of dMn compared to the lithogenic ratio observed in the total dissolvable fraction.

Neither dMn nor dFe correlated well with dSi. Throughout the whole dataset, dSi concentrations were low. Only 7 of 478 samples had dSi concentrations $> 10\,\mu M$, only 9.4 % of samples had concentrations $> 1.0\,\mu M$, and 48 % of all samples were below the limit of detection. Dissolved Si therefore had concentrations and a distribution much more like $NO_x^-$ and $PO_4^{3-}$ than Mn or Fe. This was not typically the case in glacier runoff close to the sites where ice was collected (Table S2 in the Supplement). With the exception of subglacial runoff collected on Doumer Island (South Bay, western Antarctic Peninsula), dSi concentrations in runoff were always high relative to both nitrate in runoff (typically $\sim 12 \times [NO_x^-]$) and the mean dSi concentration in icebergs. Doumer Island consists of a small ice cap which is likely cold-based with steep topography such that subglacial chemical weathering is probably limited.

No significant relationship was evident between $PO_4^{3-}$ and $NO_x^-$ concentrations, whereas a weak but significant relationship was evident between dSi and $NO_x^-$ concentrations (Fig. 3). A subset of samples appeared to show a nearly 1 : 1 relationship between dSi and $NO_x^-$, which resembles the Redfield ratio (Redfield, 1934). A closer inspection of these points shows they accounted for about 14 % of the sub-dataset where all macronutrient concentrations were detectable ($n = 22$ for those with [$NO_x^-$] and [dSi] $> 0.4\,\mu M$; for lower concentrations it is largely arbitrary in determining whether or not samples can be assigned to the group). Samples in this group include multiple catchments but with a large component from Ilulissat (32 % of data points) and Nuup Kangerlua (55 % of data points), both of which were over-represented compared to their proportional importance in the sub-dataset where they each constituted 18 % of data points. Antarctic samples and samples from Eqip Sermia were under-represented in this $\sim 1 : 1$ group, accounting for zero and two (9 %) samples, respectively, despite contributing 26 % and 20 % of the samples with all macronutrients detectable. The $\sim 1 : 1$ data points all refer to summertime, so they cannot easily be explained as mistaken sea ice samples. Furthermore, observed nutrient concentrations were often too high to be explained by carry-over from seawater contamination (see Sect. 3.2). The ratios of dSi : $NO_3^-$ also did not consistently match the ratio in near-surface fjord water samples where this was collected in parallel with icebergs. Whilst the dSi : $NO_3^-$ ratio in most near-surface samples from the Ilulissat Icefjord in August 2022 was $\sim 1$

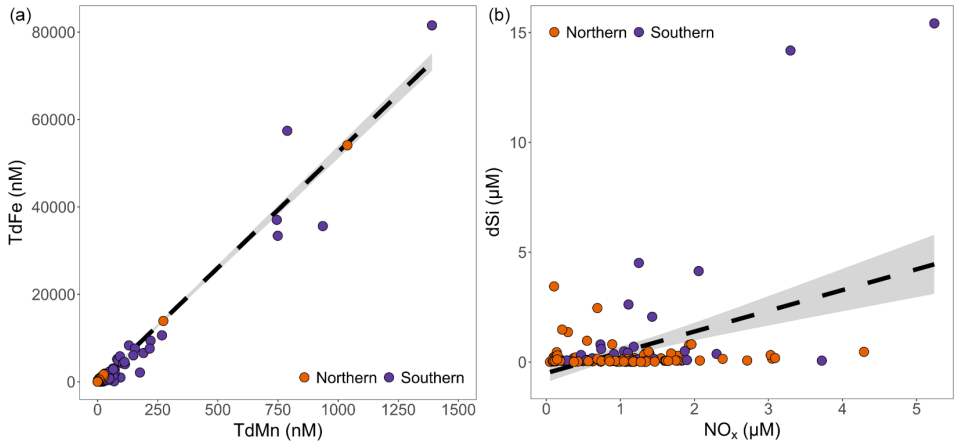


**Figure 3.** A comparison of (micro)nutrient concentrations in all ice fragments where concentrations were above the detection limits. **(a)** Total dissolvable Fe and total dissolvable Mn were strongly correlated ($p$ value $< 0.001$, $R^2 = 0.95$). Note that the highest 2 % of measured concentrations were excluded to avoid skewing the gradient. **(b)** dSi and $NO_x{}^-$ had a weak correlation ($p$ value $< 0.001$, $R^2 = 0.19$). The 95 % confidence interval is shaded in grey.

($1.39 \pm 0.61$, $n = 25$ in August 2022), for Nuup Kangerlua in August and September 2019 the ratio of dSi : $NO_3{}^-$ was always $> 18$ (Krause et al., 2021). A $\sim 1:1$ $NO_x{}^-$ : dSi ratio in ice nevertheless resembles a marine origin.

### 3.2 Evaluating reproducibility and potential sampling biases

Glacial ice can usually be visually distinguished from sea ice due to its distinct texture, colour, and morphology. For meltwater samples that were tested for salinity, values were always $< 0.3$ psu (practical salinity units). However, even minor traces of seawater in samples would be sufficient to impart a measurable macronutrient concentration change because ice macronutrient concentrations were generally very low compared to pelagic macronutrient concentrations in the corresponding sampling regions. This is particularly the case at the Antarctic sample sites where high macronutrient concentrations of 20–80 µM dSi, 1–2 µM $PO_4{}^{3-}$, and 10–30 µM $NO_3{}^-$ are relatively typical of marine waters (e.g. Höfer et al., 2019; Forsch et al., 2021; Trefault et al., 2021). Close to marine-terminating glaciers in the Arctic, macronutrient concentrations in near-surface waters can still be elevated relative to the low concentrations reported for ice, e.g. 1–30 µM dSi, 0.2–0.7 µM $PO_4{}^{3-}$, and 0–10 µM $NO_3{}^-$ for the inner part of Nuup Kangerlua (Krause et al., 2021; Meire et al., 2017). Thus, seawater macronutrient concentrations were generally equal to or greater than ice concentrations at the locations where ice calves.

Using the maximum observed marine macronutrient concentrations for our Antarctic sampling locations, assuming no detectable macronutrients in ice and that salinity of 0.3 exclusively reflected the carry-over of seawater from sampling, nutrient concentrations of up to 0.26 µM $NO_3{}^-$, 0.02 µM $PO_4{}^{3-}$, and 0.069 µM dSi could be observed as a seawater contamination signal. The rinsing procedure used to collect samples herein, whereby ice was sequentially melted, with the meltwater then used to swill and rinse the sample bag, was designed to minimize trace metal contamination, and three such rinses undertaken correctly would theoretically remove $\sim 99.99$ % of any saline water collected with an ice sample in addition to any contamination from ice handling. This would also not leave a detectable ($> 0.01$) salinity increase in the collected sample such that any detected salinity would have to come from ice melt. Sea ice samples were not targeted for sampling herein, but two samples were collected during the 2017 Pia Fjord campaign (Patagonia) alongside calved ice samples with measured macronutrient concentrations of 2.00 and 5.97 µM $NO_x{}^-$, 0.08 and 0.13 µM $PO_4{}^{3-}$, and 0.28 and 0.63 µM dSi. These sea ice $NO_x{}^-$ and dSi concentrations were above average compared to freshwater ice samples collected at the same location (Table S2). Similarly, samples of land-fast sea ice from Antarctica generally have high concentrations of all macronutrients compared to iceberg samples reported herein (Grotti et al., 2005; Günther and Dieckmann, 1999; Nomura et al., 2023). The ratio of $NO_x{}^-$ : $PO_4{}^{3-}$ : dSi in sea ice is strong evidence that nutrients in sea ice have a primarily saline origin (Henley et al., 2023). Sampling protocols for sea ice are however different in several aspects, particularly the application of sequential rinsing (for glacial ice but not for sea ice) and ambient temperatures during sample collection. A sequential rinsing with sea ice, as applied herein, might lead to an uneven distribution of nutrients in meltwater samples due to the layered structure of sea ice and the effects of brine channels (Ackley and Sullivan, 1994; Gleitz et al., 1995; Vancoppenolle et al., 2010). With the possible exceptions of regions that experience ice mélange (a mixture of sea ice and icebergs) and/or

marine ice, glacial ice is expected to be more homogenous with respect to salinity.

During the dedicated iceberg cruise campaign GLICE in Disko Bay (August 2022), ice collection was confined to four subregions of interest (Fig. 4, Table S3 in the Supplement). There was partial ice cover in Disko Bay during boreal summer, which was mainly limited to a patch of high iceberg density close to the outflow of Ilulissat Icefjord. Combined with the confined nature of the coastal fjords sampled and the relatively fast disintegration of smaller ice fragments, it was possible to identify with a high degree of certainty the origin of ice within each subregion (Fig. 4). Within the fjord system hosting the marine-terminating glacier Eqip Sermia, ice fragments were highly likely to have originated either from Eqip Sermia itself or, if not, from adjacent calving fronts in the same fjord. Similarly, close to the outflow of Ilulissat Icefjord, ice fragments were highly likely to have originated from Sermeq Kujalleq. Ice slicks which were visibly observed to calve from two offshore icebergs within an hour prior to sample collection each constituted an additional subregion of interest. The two icebergs, referred to herein as Narwhal and Beluga, were both isolated from other floating ice features with maximum dimensions above the waterline of $> 100$ m width and $> 20$ m height (Fig. 4). Radar measurements determined that Narwhal was approximately stationary throughout the observation period ($\sim 12$ h), likely pirouetting on an area of shallow bathymetry. The Beluga iceberg was free-floating and proceeding northwards along a trajectory through the area which hosted the highest observed iceberg densities in Disko Bay over the cruise duration (mid-August 2022).

Ice from the four sampled subregions in Disko Bay was similar in all cases with overlapping ranges for the $NO_x{}^-$, $PO_4{}^{3-}$, and dSi concentrations of ice at different locations (Fig. 5). A PERMANOVA analysis showed small but significant differences ($R^2 = 0.15$, $p$ value $= 0.002$) in the chemical composition of iceberg samples collected inshore (groups A and C, Fig. 4) or offshore (groups B and D, Fig. 4) in Disko Bay when combining groups. An ordination analysis (nMDS stress $= 0.04$) showed that offshore icebergs were grouped together on the left side of the ordination, whereas inshore icebergs were more common on the right side of the ordination (Fig. 5). In general, offshore and inshore icebergs presented similar concentrations of all nutrients in most of the samples, except for a few inshore samples that had higher concentrations of all nutrients (Fig. 5). When testing these differences for each individual nutrient, only $PO_4{}^{3-}$ showed significant differences between the two categories ($p$ value $=$ 0.035), with offshore icebergs showing lower concentrations (Fig. 5). The difference between inshore and offshore ice, whilst present, was therefore relatively modest.

Further insight can be gained from a comparison of all data available from Nuup Kangerlua, a relatively well-studied glacier fjord in southwestern Greenland. The fjord hosts three marine-terminating glaciers with heavy ice mélange cover observed in the inner fjord year-round and some sea ice in the inner fjord during winter. Samples were collected from the fjord during five independent field campaigns from 2014 to 2019 in different seasons from May in boreal spring to September in boreal autumn. Considering the number of parameters sampled and the relatively high standard deviation of almost all parameters relative to the mean or median measured concentrations, there was limited evidence for any seasonal or inter-campaign differences (Table S4). No significant differences ($p > 0.05$) were found between groups of samples obtained at the same field site when organizing the complete dataset by field site and defining each separate field campaign as a group.

### 3.3 Sediment load within icebergs and its relationship with nutrient concentration

The sediment load within icebergs collected around the Antarctic Peninsula was highly variable with a maximum of $5072\,\mathrm{mg\,L^{-1}}$ and a minimum of $0.69\,\mathrm{mg\,L^{-1}}$ (median of $8.5\,\mathrm{mg\,L^{-1}}$, mean of $430.5\,\mathrm{mg\,L^{-1}}$). Particle loads were assessed at three Antarctic locations. The median dry mass was similar across the three areas, but the mean ($\pm$ standard deviation) dry mass was more variable due to the occasional sample with a high sediment load. Mean dry masses across the three areas were $910 \pm 6300\,\mathrm{mg\,L^{-1}}$ for Maxwell Bay, King George Island ($n = 65$); $35 \pm 110\,\mathrm{mg\,L^{-1}}$ for Thunder Bay and Neumayer Channel, Wiencke Island ($n = 19$); and $39 \pm 98\,\mathrm{mg\,L^{-1}}$ for South Bay, Doumer Island ($n = 60$). Median sediment loads in the three regions were 12, 2.5, and $7.7\,\mathrm{mg\,L^{-1}}$, respectively. The heterogeneous distribution of sediments was reflected in the fact that $\sim 2\,\%$ of samples collected contributed $\sim 90\,\%$ of the total sediment retrieved from the iceberg samples collectively. This distribution is similar to previous analysis regarding TdFe (Hopwood et al., 2019) and sediment load in icebergs from Svalbard (Dowdeswell and Dowdeswell, 1989). It also qualitatively matches the distribution of TdMn and TdFe observed herein (see Sect. 3.1).

As Fe, Mn, and dSi might have sedimentary origins, we tested if there were any significant relationships between the sediment load of an iceberg and the concentration of each macronutrient and both total dissolvable and dissolved trace metals (Fig. 6). For $NO_x{}^-$ and $PO_4{}^{3-}$ there was no significant relationship between sediment load and concentration ($p$ values of 0.18 and 0.26, respectively). Conversely, TdFe, TdMn, dFe, dMn, and dSi all had significant relationships with sediment load. The concentrations of the total dissolvable fraction of trace metals showed better fits (TdFe $R^2 = 0.43$, $p$ value $< 0.001$; TdMn $R^2 = 0.43$, $p$ value $<$ 0.001) than the dissolved phases of metals (dFe $R^2 = 0.30$, $p$ value $< 0.001$; dMn $R^2 = 0.20$, $p$ value $< 0.001$) and dSi ($R^2 = 0.28$, $p$ value $< 0.001$). This is consistent with the expectation that englacial sediment leads to direct enrichment in TdFe and TdMn, which increase proportionately with the

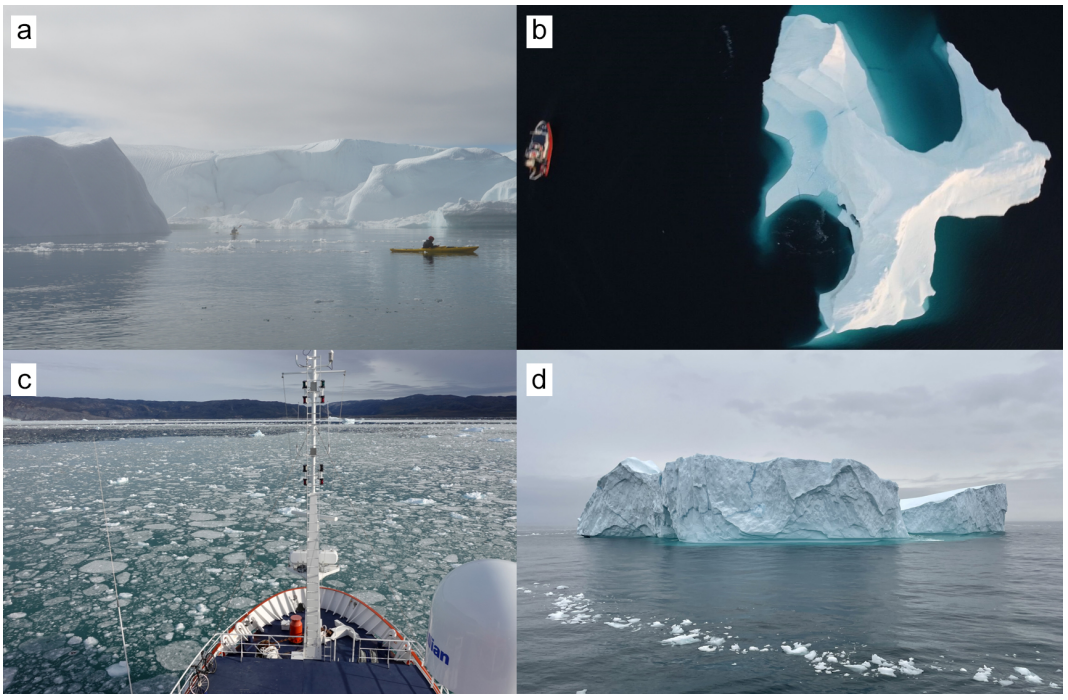


**Figure 4.** Ice sample collection areas in four distinct regions of Disko Bay. **(a)** Icebergs grounded on the sill at the entrance to the Ilulissat Icefjord. **(b)** An offshore iceberg which was grounded during the sampling period referred to herein as the Narwhal iceberg. **(c)** Ice fragments in front of the marine-terminating glacier Eqip Sermia. **(d)** An offshore iceberg which was free-floating during the sampling period referred to herein as the Beluga iceberg.

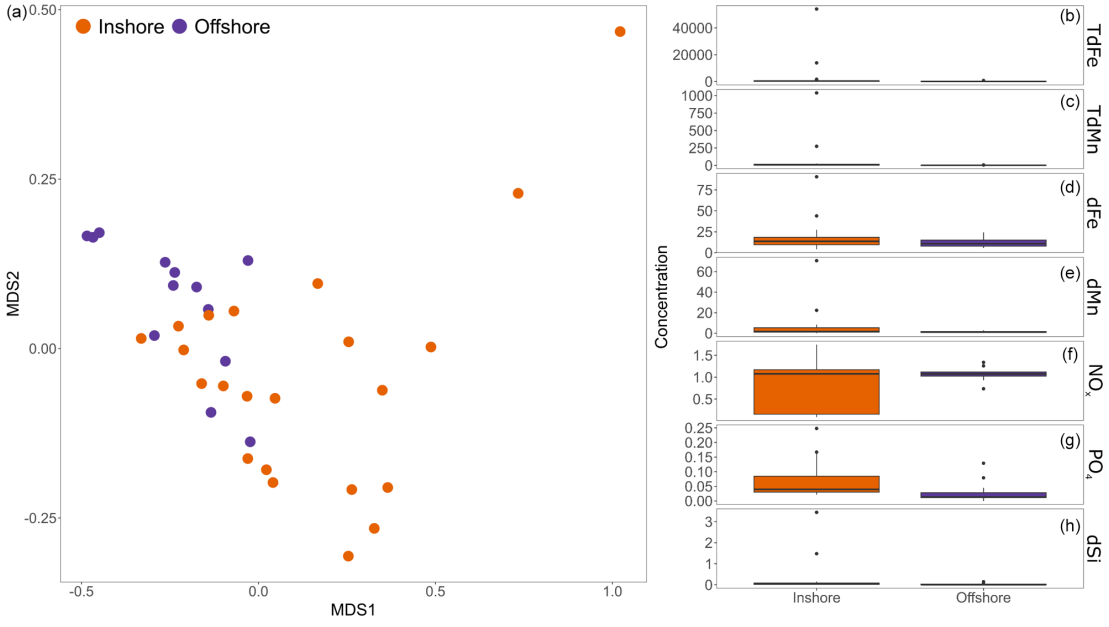


**Figure 5.** Comparison of nutrient concentrations from inshore and offshore ice samples collected at Disko Bay (August 2022; see Fig. 4). **(a)** An ordination analysis (nMDS) comparing concentrations of all nutrients measured in ice, contrasting inshore and offshore areas of Disko Bay. Inshore samples were collected within 1 km of the coastline, whereas offshore values were all from > 15 km away from the coastline. A PERMANOVA analysis of iceberg nutrient concentrations showed weak but significant differences between both areas ($R^2 = 0.15$, $p$ value $= 0.002$). **(b–h)** A direct comparison of all nutrient concentrations for the same dataset. Units are micromoles per litre (µM) for dSi, $NO_x{}^-$, and $PO_4{}^{3-}$ and nanomoles per litre (nM) for all trace metals. Only $PO_4{}^{3-}$ showed a significant difference between the two categories ($p$ value $= 0.035$).

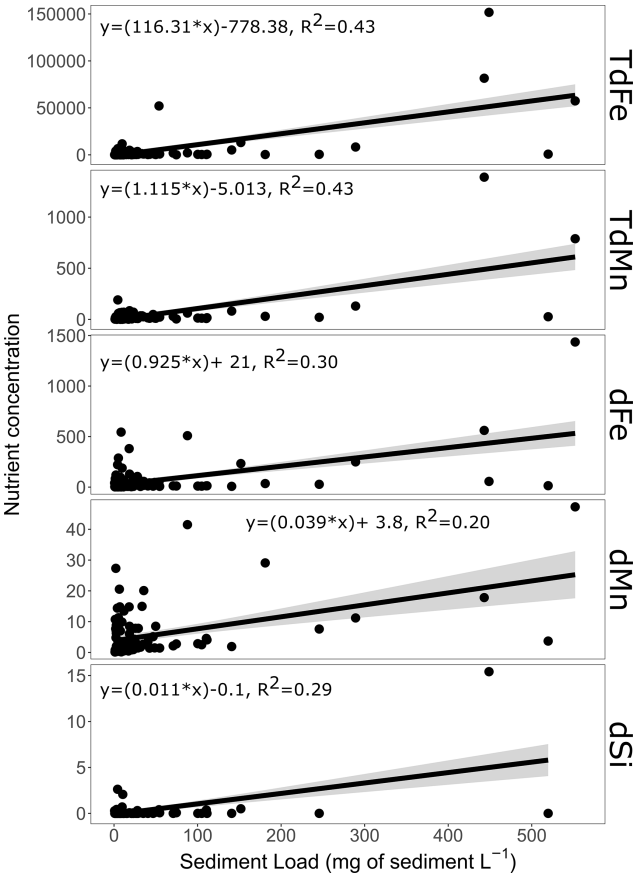


**Figure 6.** Iceberg sediment load and its relationship with nutrient concentrations. The relationship between nutrient concentrations and sediment load for ice samples from the Antarctic Peninsula (no samples from elsewhere determined sediment load of the same ice fragments as nutrient concentrations). Only significant ($p$ value $< 0.001$) relationships are shown. No significant relationship was evident for the sediment load with nitrate or phosphate. Units are micromoles per litre (µM) for dSi and nanomoles per litre (nM) for all trace metals.

sediment load. The enrichment of dFe, dMn, and dSi is more variable and may depend on the specific conditions that sediment and ice experience between englacial sediment incorporation and sample collection.

On several occasions in Nuup Kangerlua and Maxwell Bay we observed structures up to several centimetres wide/deep on iceberg surfaces akin to cryoconite holes both above and below the waterline. The sediment within such holes was easily disturbed. The regular agitation and movement of floating ice fragments and the chaotic nature of calving events suggests that cryoconite holes on icebergs formed in situ rather than being relics of a glacier surface prior to calving. This raises an interesting question about whether sediment-rich layers and any associated nutrients could be subject to disintegration mechanisms distinct from bulk ice. When large ice samples weighing 10–45 kg were stored in the dark at 5–10 °C, higher loads of sediment were released in the initial melt fractions (Fig. S1 in the Supplement). This trend was highly reproducible, occurring in all observed experiments ($n = 8$) when large ice samples specifically targeted for their high englacial sediment loads were retained. The sediment release rate declined with an exponential logarithmic function over the first 48 h (Fig. S1). It should be noted that randomly collected samples had much lower sediment loads.

## 4 Discussion

### 4.1 Insights into nutrient origins from ratios

There are several distinct mechanisms via which ice could accumulate different nutrient ratios. Precipitation and aerosol deposition on ice surfaces will contribute to the $NO_x^-$ and $PO_4^{3-}$ concentrations present in the ice matrix (Fischer et al., 1998; Kjær et al., 2015), assuming a limited biogeochemical imprint from surface biological (or photochemical) processes. Phosphate concentrations in ice from the last glacial period in Greenland are reported to range from 3 to 62 nM (Kjær et al., 2015). These ranges are similar to the $NO_3^-$ and $PO_4^{3-}$ values we report for Greenlandic calved ice herein: mean (± standard deviation) of $0.78 \pm 0.69$ $NO_3^-$, median of 0.74 $NO_3^-$, mean of $36 \pm 50$ nM $PO_4^{3-}$, and median of 28 nM $PO_4^{3-}$. Modern atmospheric deposition is expected to impact the N : P ratio as atmospheric pollution is generally associated with higher N : P ratios (e.g. Peñuelas et al., 2012) and could explain the increase in the N : P ratio at higher $NO_3^-$ concentrations. Antarctica is less directly affected by anthropogenic emissions, but the ranges of $NO_3^-$ reported for snow and ice samples overlap with the corresponding values for Greenland, e.g. ranges of 0.08–2.12 µM (Akers et al., 2022) and 0.29–2.58 µM (Neubauer and Heumann, 1988).

In addition to macronutrient concentrations in the ice matrix, some degree of sedimentary signal might also affect dSi concentrations due to the release of dSi from glacier-associated weathering processes (Halbach et al., 2019; Wadham et al., 2010). Sediment associated with an iceberg could be from basal layers or other englacial sediment entrained prior to calving or acquired from scouring events subsequent to calving. Shallow areas of all field sites herein had grounded icebergs. In Disko Bay during 2 weeks of cruise observations in August 2022 for example, the majority of large (> 100 m width above the water line) icebergs were observed to be grounded. In terms of TdFe, TdMn, dFe, dMn, and dSi we hypothesize that two categories of sediment may be distinguishable. Englacial sediment with little biogeochemical processing should retain a TdFe : TdMn ratio which is close to the crustal abundance ratio of Fe : Mn, with low dFe, dMn, and dSi concentrations. Basal sediment layers, particularly from catchments with warm-based glaciers, may have a similar TdFe : TdMn ratio but higher concentra-

tions of dFe, dMn, and dSi due to more active biogeochemical processing in subglacial environments (e.g. Wadham et al., 2010; Tranter et al., 2005). Finally, scoured sediments acquired after calving could constitute a broad range of compositions considering the gradient in benthic conditions along glacier fjords (Laufer-Meiser et al., 2021; Wehrmann et al., 2013) and may accordingly contain more biogenic and/or authigenic phases than englacial sediment. These sediments may be highly variable in composition but should impart high TdFe and TdMn concentrations, with varying Fe : Mn ratios, and high dFe, dMn, and dSi concentrations. Basal sediments and scoured sediments from fjord environments therefore probably cannot be distinguished unambiguously from concentrations measured herein alone. Yet we can likely distinguish englacial sediment from basal or scoured sediment. Dissolved Si concentrations were low across the whole dataset, suggesting basal ice was a very small component of sampled ice. The linear relationship between TdFe and TdMn across a wide range of observed concentrations also suggests minimal incorporation of authigenic mineral phases and, in combination with low dSi, hints at basal ice from warm-based glaciers being largely absent from this dataset. This is consistent with the expectation that basal layers are largely lost prior to or rapidly following iceberg calving (Smith et al., 2019). In contrast, in runoff sampled close to iceberg sampling regions, dSi concentrations were elevated (range of 1.2–44 µM) and often considerably higher than concentrations measured in ice melt (Table S2).

The weak but significant relationships with dSi, dFe, dMn, and sediment load and the stronger relationships between TdFe and TdMn and sediment load are consistent both with a sedimentary origin of these components and the caveats that further physical and/or biogeochemical processing mechanisms have to be considered to fully explain the distributions of dSi, dFe, and dMn (Fig. 6). As the concentrations of $NO_x{}^-$ and $PO_4{}^{3-}$ were consistent with an ice matrix origin, a varying concentration of dSi from sedimentary sources could also explain the observed trend in the $NO_x{}^-$ : dSi and $PO_4{}^{3-}$ : dSi ratios. Whilst elevated dFe and dMn concentrations in runoff reflect release of these phases from glacier-derived sediments (Hawkings et al., 2020; Raiswell, 2011), the concentrations herein for ice melt were not strongly correlated with each other or sediment load (Fig. 6). This could reflect the origin of dissolved Fe and Mn from distinct, different mineral phases. Yet dFe concentrations generally correlate poorly with other trace elements in aquatic environments due to rapid scavenging onto particle surfaces and rapid aggregation of colloids (which are included within the "$< 0.2$ µm" definition of dissolved herein) (Zhang et al., 2015). A poor correlation could also therefore reflect the tendency for inorganic dFe species to become rapidly scavenged close to source (Lippiatt et al., 2010). Measured concentrations herein refer to freshly collected meltwater, so it is difficult to establish how dFe concentrations may have changed during the ice-melting process. Conversely, dMn species are more stable in solution, especially in the photic zone (Sunda et al., 1983; Sunda and Huntsman, 1988), and this is often reflected in much higher dMn : dFe ratios in proglacial aquatic environments than would be expected based on crustal abundances (e.g. van Genuchten et al., 2022; Hawkings et al., 2020; Yang et al., 2022). Curiously, dSi also correlated poorly with all metal phases. This again could simply reflect different mineral phases driving elevated dSi, dFe, and dMn concentrations (van Genuchten et al., 2022). Yet considering all of these elements (Si, Fe, and Mn) are expected to be released from labile phases present in glacier-derived sediments, at least within specific regions some degree of correlation might be expected. Further work to quantify the rates of gross and net dFe, dMn, and dSi release under in situ conditions within ice and frozen sediment layers could perhaps elucidate processes via which net release of these components may be uncoupled. Photochemical processes are particularly likely to affect Fe and Mn release (Kim et al., 2010, 2024), and the scavenging potential of Mn and Fe species (van Genuchten et al., 2022) may also be important in terms of how they interact with other dissolved and particulate components of the ice–sediment–meltwater matrix.

### 4.2 Key role of sediment-rich layers and their disintegration for nutrient release

Several works have speculated that Arctic and Antarctic icebergs may have distinct differences in sediment load, with the former generally having higher sediment loads (Anderson et al., 1980). However, there are several observer biases in making such comparisons. Arctic icebergs are generally smaller because they are typically sourced from tidewater glacier fronts rather than calved from larger ice shelves. Arctic icebergs are also logistically easier to observe and access compared to Antarctic icebergs. A comparison of smaller ice fragments from Kongsfjorden in Svalbard and three localities in the Antarctic Peninsula showed that the former had higher sediment loads. Mean sediment loads of 21 g $L^{-1}$ (median of 0.58 g $L^{-1}$) were previously reported for Kongsfjorden (Hopwood et al., 2019). Average sediment load values for ice fragments handled similarly from the Antarctic Peninsula were 8.5 mg $L^{-1}$ (median) and 430.5 mg $L^{-1}$ (mean), respectively, which are considerably lower. Contrasting warm-/cold-based glaciers and the higher ratio of exposed land to ice cover of the coastal glaciated Arctic may explain much of this difference.

Sediment-rich layers within icebergs have long been hypothesized to be particularly important for the delivery of the micronutrient Fe into the ocean (Hart, 1934), and this has been explicitly confirmed with measurements of dFe and particulate Fe (Lin et al., 2011; Raiswell, 2011). We verify herein that sediment distribution is a major factor explaining TdFe and TdMn distribution yet suggest this is a less important factor in explaining dFe, dMn, and dSi distribution in icebergs (Fig. 6). The dynamics of sediment-rich layers

and their fate in the marine environment is of special interest for trace metal biogeochemistry given the (co-)limiting role these micronutrients have for phytoplankton growth in the Southern Ocean (Hawco et al., 2022; Martin et al., 1990b). Yet multiple factors are likely important for determining the delivery of dFe and dMn to the marine environment because these fluxes do not simply scale with sediment input as for TdFe and TdMn. A close association of TdFe and TdMn is perhaps unsurprising and corroborates a lithogenic origin for the vast majority of Fe present in icebergs. It also suggests limited biogeochemical processing of englacial material and/or rapid loss of basal ice layers preventing the modification of a lithogenic ratio in between sediment acquisition by icebergs and sediment release in the ocean (Forsch et al., 2021).

A further, to our knowledge, novel observation was the tendency of embedded sediment to be rapidly discharged from ice fragments. When collecting larger pieces of ice it was found that, in all cases, embedded sediment was rapidly washed out of the ice fragments largely within the melting of the first 10 %–20 % of ice volume (Fig. S1). These ice fragments were specifically targeted to avoid ice with surface sediment layers, and so this result cannot be explained by the loss of sediment frozen on the surface of ice. If this process was occurring at larger scales in nature, it could further act to skew the deposition of iceberg-borne particles towards inshore environments; i.e. it would compound the inefficiencies in the delivery of sediment and associated nutrients to the offshore marine environment due to the rapid loss of basal ice layers. The mechanism of this process is unclear.

### 4.3 (Micro)nutrient fluxes to the ocean from icebergs

By combining measured concentrations herein with estimates of the ice volume discharged from Greenland and Antarctica, annual flux estimates can be estimated for (micro)nutrients associated with icebergs (Table 1). For the macronutrients $NO_3^-$, $PO_4^{3-}$, and dSi, the uncertainty in these flux estimates remains large relative to the magnitude of the flux. This is an inherent result of the large fraction of ice with macronutrient concentrations close to the LOD, so it would not be changed with further data collection. Iceberg-derived macronutrient fluxes are likely minor in terms of annual polar pelagic nutrient cycling (Table 1) and in most coastal environments will dilute, rather than enhance, ambient macronutrient concentrations. This is especially the case in Antarctic waters, where macronutrient concentrations are universally high (Garcia et al., 2018). The low macronutrient level of ice also implies that physical effects associated with iceberg passage, mixing, and any stratification resulting from meltwater likely have larger effects on annual macronutrient budgets for biota than the direct contribution of meltwater (Helly et al., 2011; Tarling et al., 2024). In regions where meltwater from icebergs accumulates in a thin surface layer, which is a phenomenon largely confined to Arctic fjords (e.g. Enderlin et al., 2016), low macronutrient concentrations may contribute to low primary production in near-surface layers. Although it should be noted that meltwater delivery is not confined to the surface (Moon et al., 2018) and, as noted, can drive the vertical entrainment of macronutrients within the water column.

**Table 1.** Annual fluxes of nutrients associated with icebergs assuming calved ice volumes of $500\,km^3\,yr^{-1}$ from Greenland and $1100\,km^3\,yr^{-1}$ from Antarctica (Bamber et al., 2018; Rignot et al., 2013). Values are the mean ± standard deviation (median); "b/d" represents a median sample below the limit of detection.

| Nutrient | Greenland ice sheet annual discharge ($Mmol\,yr^{-1}$) | Antarctic ice sheet annual discharge ($Mmol\,yr^{-1}$) |
|---|---|---|
| $NO_3^-$ | 389 ± 345 (370) | 418 ± 796 (168) |
| $PO_4^{3-}$ | 18 ± 25 (14) | 76 ± 83 (58) |
| dSi | 212 ± 701 (27) | 476 ± 2187 (b/d) |
| dFe | 7.1 ± 15 (3.9) | 130 ± 472 (18) |
| dMn | 2.3 ± 6.0 (0.77) | 32 ± 191 (3.3) |

Delivery of total dissolvable Fe and Mn fluxes from icebergs to the ocean may be considerable (Table 1), but, as these components are associated with heterogeneous particle-rich layers in ice, their delivery may be skewed towards inshore waters where primary production is less limited by trace metal availability. Dissolved Fe and Mn components are more directly relevant to phytoplankton demands on the short-term timescales associated with iceberg passage, due to the short residence time of particle-associated metal phases in the marine environment. Annual dFe and dMn fluxes also carry relatively large uncertainties (Table 1) which reflect the wide range of concentrations present in ice. Although the crustal abundance of Mn oxides is approximately 50× lower than that of Fe oxides (Rudnick and Gao, 2004), dMn fluxes from Greenland and Antarctica are 32 % and 25 % of the corresponding dFe fluxes, respectively (Table 1). Similar trends are evident in dFe and dMn concentrations within fjord environments where trace metals from subglacial discharge and runoff enter the ocean (Forsch et al., 2021; van Genuchten et al., 2022). The relatively high concentrations of dMn compared to dFe likely reflect the rapid scavenging of dFe close to the source compared to more conservative behaviour of dMn over short (hours to days) timescales (Kandel and Aguilar-Islas, 2021; Yang et al., 2022; Zhang et al., 2015).

A key finding throughout was that the macronutrient and micronutrient content of ice was relatively similar between catchments and regions worldwide despite the contrasting geographic context of Arctic and Antarctic ice calving fronts and notable differences in sediment loads between regions (Fig. 2). There was limited evidence of differences in ice nutrient concentrations between field campaigns returning to the same location (Nuup Kangerlua, southwestern Green-

land) in different seasons/years and similarly limited evidence of differences contrasting ice fragments collected offshore in Disko Bay (western Greenland) with ice fragments collected inshore close to marine-terminating glacier fronts (Fig. 5). Icebergs are inherently heterogenous due to the nature of englacial and basal sediment incorporation and loss processes. This heterogeneity combined with generally low nutrient concentrations appears to mask any regional or catchment-specific trends in macronutrient or micronutrient content related to changing bedrock composition (e.g. Halbach et al., 2019), calving dynamics (Smith et al., 2019), or photochemical processes (e.g. Kim et al., 2010).

Whilst further sampling would not reduce uncertainty in the estimated nutrient fluxes (Table 1), some specific caveats with our present work could be resolved in the future. Herein we have considered only $NO_x^-$ and $PO_4^{3-}$ as sources of bioaccessible nitrogen and phosphorous, but considering the universally low concentrations present in icebergs, other N and P sources (e.g. DON, dissolved organic nitrogen; DOP, dissolved organic phosphorous; and $NH_4$) may be relatively important (Parker et al., 1978). We hypothesized that a basal ice influence would be present in some ice fragments with high dSi alongside dFe and dMn but conversely found very low dSi concentrations across all field locations. Future process studies might elucidate the mechanistic reasons why elevated dSi concentrations are not present alongside dFe and dMn concentrations in ice melt. Finally, sediment-rich layers of large ice samples were observed to rapidly melt, potentially indicating that these layers are prone to disintegration. Such a mechanism could be an important regulator of sediment dispersion in the marine environment, potentially further skewing the delivery of iceberg-rafted debris and nutrients towards coastal waters.

## 5 Conclusions

The dataset reported here covers ice fragments collected from a range of Arctic and Antarctic polar and subpolar marine-terminating glaciers and floating ice tongues. Throughout, icebergs are found to be only a minor source of macronutrients to the ocean with a large fraction of measurements close to or below the standard analytical detection limit, especially for $PO_4^{3-}$ and dSi. Icebergs do however deliver modest fluxes of dissolved Fe and Mn to the polar oceans, which are likely important ecologically, particularly in the Southern Ocean (Sedwick et al., 2000; Wu et al., 2019). The rapid dilution of meltwater close to icebergs, typically to concentrations $< 1\,\%$ (Helly et al., 2011; Stephenson et al., 2011), means these trace metal inputs are challenging to constrain from in situ pelagic observations (Lin et al., 2011); thus our measurements provide a first-order constraint on iceberg-derived micronutrient fluxes going into polar seas. The scavenged-type behaviour of dFe may explain why the dMn : dFe ratio in ice melt is considerably higher than expected from crustal abundances of Fe and Mn oxides, yet this also raises questions about how micronutrients sourced from icebergs behave immediately after release into the ocean. Dissolved Fe may be scavenged close to the source, limiting the spatial extent of Fe fertilization from iceberg tracks, whereas, especially in the photic zone, dMn is more stable in seawater (Sunda et al., 1983). Thus icebergs may be an even more disproportionately important dMn source to biota than the dFe : dMn ratio in meltwater suggests.

*Data availability.* New data presented herein are available from SeaDataNet (https://emodnet.ec.europa.eu/geonetwork/emodnet/api/records/ff3c625c-6a39-46ef-b329-222040f85917, Hopwood et al., 2023). Literature data were compiled from priorly published values (De Baar et al., 1995; Campbell and Yeats, 1982; Forsch et al., 2021; Höfer et al., 2019; Hopwood et al., 2017, 2019; Lin et al., 2011; Loscher et al., 1997; Martin et al., 1990b). For convenience, a merged Supplement is appended for data not previously compiled.

*Supplement.* The supplement related to this article is available online at: https://doi.org/10.5194/tc-18-5735-2024-supplement.

*Author contributions.* MJH, DC, JH, and EPA designed the study and acquired funding and resources. JK, DC, JD, JH, EA, TL, LM, and MJH conducted fieldwork. EA, KZ, and MJH conducted laboratory analysis. JK, JH, and MJH conducted data analysis. JK and MJH wrote the initial draft of the paper, and all authors contributed to revision of the text.

*Competing interests.* The contact author has declared that none of the authors has any competing interests.

*Disclaimer.* Publisher's note: Copernicus Publications remains neutral with regard to jurisdictional claims made in the text, published maps, institutional affiliations, or any other geographical representation in this paper. While Copernicus Publications makes every effort to include appropriate place names, the final responsibility lies with the authors.

*Acknowledgements.* Tim Steffens (GEOMAR) is thanked for technical assistance with ICP-MS; André Mutzberg (GEOMAR) is thanked for macronutrient data; and Stephan Krisch (formerly of GEOMAR), Thomas Juul-Pedersen (Greenland Institute of Natural Resources, GINR), and Case van Genuchten (Geological Survey of Denmark and Greenland, GEUS) are thanked for assistance with sampling. The captain and crew of R/V *Sanna* are thanked for field support. Jeremy Donaire was sponsored by a scholarship from the Instituto Antártico Chileno (INACH), Correos de Chile, and the Fuerza Aérea de Chile (FACH). Ship time and work in Nuup Kangerlua were conducted in collaboration with MarineBasis Nuuk, part of the Greenland Ecosystem Monitoring (GEM) project. We gratefully acknowledge logistics and funding contributions from

the Danish Center for Marine Research (DCH), the Greenland Institute of Natural Resources, the Novo Nordisk Foundation (grant no. NNF17SH0028142), and INACH.

*Financial support.* This research has been supported by the Fondo de Financiamiento de Centros de Investigación en Áreas Prioritarias (grant no. FONDAP-IDEAL 15150003), the Fondo Nacional de Desarrollo Científico y Tecnológico (grant no. 1211338), the Deutsche Forschungsgemeinschaft (grant no. HO 6321/1-1), the Swiss Polar Institute (grant no. GLACE), the National Natural Science Foundation of China (grant no. 42150610482), the European Union H2020 research and innovation programme (grant no. 824077), the Nederlandse Organisatie voor Wetenschappelijk Onderzoek (grant no. 016.Veni.192.150), and the Novo Nordisk Fonden (grant no. NNF17SH0028142).

*Review statement.* This paper was edited by Elizabeth Bagshaw and reviewed by two anonymous referees.

## References

Ackley, S. F. and Sullivan, C. W.: Physical controls on the development and characteristics of Antarctic sea ice biological communities – a review and synthesis, Deep-Sea Res. Pt. I, 41, 1583–1604, https://doi.org/10.1016/0967-0637(94)90062-0, 1994.

Akers, P. D., Savarino, J., Caillon, N., Servettaz, A. P. M., Le Meur, E., Magand, O., Martins, J., Agosta, C., Crockford, P., Kobayashi, K., Hattori, S., Curran, M., van Ommen, T., Jong, L., and Roberts, J. L.: Sunlight-driven nitrate loss records Antarctic surface mass balance, Nat. Commun., 13, 4274, https://doi.org/10.1038/s41467-022-31855-7, 2022.

Alley, R. B., Cuffey, K. M., Evenson, E. B., Strasser, J. C., Lawson, D. E., and Larson, G. J.: How glaciers entrain and transport basal sediment: Physical constraints, Quaternary Sci. Rev., 16, 1017–1038, https://doi.org/10.1016/S0277-3791(97)00034-6, 1997.

Anderson, J. B., Domack, E. W., and Kurtz, D. D.: Observations of Sediment–laden Icebergs in Antarctic Waters: Implications to Glacial Erosion and Transport, J. Glaciol., 25, 387–396, https://doi.org/10.3189/S0022143000015240, 1980.

Bamber, J. L., Tedstone, A. J., King, M. D., Howat, I. M., Enderlin, E. M., van den Broeke, M. R., and Noel, B.: Land Ice Freshwater Budget of the Arctic and North Atlantic Oceans: 1. Data, Methods, and Results, J. Geophys. Res.-Oceans, 123, 1827–1837, https://doi.org/10.1002/2017JC013605, 2018.

Boyd, P. W., Arrigo, K. R., Strzepek, R., and Van Dijken, G. L.: Mapping phytoplankton iron utilization: Insights into Southern Ocean supply mechanisms, J. Geophys. Res.-Oceans, 117, C06009, https://doi.org/10.1029/2011JC007726, 2012.

Browning, T. J., Achterberg, E. P., Engel, A., and Mawji, E.: Manganese co-limitation of phytoplankton growth and major nutrient drawdown in the Southern Ocean, Nat. Commun., 12, 884, https://doi.org/10.1038/s41467-021-21122-6, 2021.

Campbell, J. A. and Yeats, P. A.: The distribution of manganese, iron, nickel, copper and cadmium in the waters of Baffin Bay and the Canadian Arctic Archipelago, Oceanol. Acta, 5, 161–168, https://doi.org/10.1007/s00128-002-0077-7, 1982.

Cook, J., Edwards, A., Takeuchi, N., and Irvine-Fynn, T.: Cryoconite: The dark biological secret of the cryosphere, Progress in Physical Geography: Earth and Environment, 40, 66–111, https://doi.org/10.1177/0309133315616574, 2015.

Craven, M., Allison, I., Fricker, H. A., and Warner, R.: Properties of a marine ice layer under the Amery Ice Shelf, East Antarctica, J. Glaciol., 55, 717–728, https://doi.org/10.3189/002214309789470941, 2009.

De Baar, H. J. W., De Jong, J. T. M., Bakker, D. C. E., Loscher, B. M., Veth, C., Bathmann, U., and Smetacek, V.: Importance of iron for plankton blooms and carbon dioxide drawdown in the Southern Ocean, Nature, 373, 412–415, https://doi.org/10.1038/373412a0, 1995.

Dowdeswell, J. A. and Dowdeswell, E. K.: Debris in Icebergs and Rates of Glaci-Marine Sedimentation: Observations from Spitsbergen and a Simple Model, J. Geol., 97, 221–231, https://doi.org/10.1086/629296, 1989.

Enderlin, E. M., Hamilton, G. S., Straneo, F., and Sutherland, D. A.: Iceberg meltwater fluxes dominate the freshwater budget in Greenland's iceberg-congested glacial fjords, Geophys. Res. Lett., 43, 287–294, https://doi.org/10.1002/2016GL070718, 2016.

Fischer, H., Wagenbach, D., and Kipfstuhl, J.: Sulfate and nitrate firn concentrations on the Greenland ice sheet: 1. Large-scale geographical deposition changes, J. Geophys. Res.-Atmos., 103, 21927–21934, https://doi.org/10.1029/98JD01885, 1998.

Fischer, H., Schüpbach, S., Gfeller, G., Bigler, M., Röthlisberger, R., Erhardt, T., Stocker, T. F., Mulvaney, R., and Wolff, E. W.: Millennial changes in North American wildfire and soil activity over the last glacial cycle, Nat. Geosci., 8, 723–727, https://doi.org/10.1038/ngeo2495, 2015.

Forsch, K. O., Hahn-Woernle, L., Sherrell, R. M., Roccanova, V. J., Bu, K., Burdige, D., Vernet, M., and Barbeau, K. A.: Seasonal dispersal of fjord meltwaters as an important source of iron and manganese to coastal Antarctic phytoplankton, Biogeosciences, 18, 6349–6375, https://doi.org/10.5194/bg-18-6349-2021, 2021.

Garcia, H. E., Weathers, K., Paver, C. R., Smolyar, I., Boyer, T. P., Locarnini, R. A., Zweng, M. M., Mishonov, A. V., Baranova, O. K., Seidov, D., and Reagan, J. R.: World Ocean Atlas 2018, Volume 4: Dissolved Inorganic Nutrients (phosphate, nitrate and nitrate+nitrite, silicate), A. Mishonov Technical Ed., NOAA Atlas NESDIS 84, 35 pp., https://www.ncei.noaa.gov/products/world-ocean-atlas (last acces: November 2024), 2018.

Gleitz, M., v.d. Loeff, M. R., Thomas, D. N., Dieckmann, G. S., and Millero, F. J.: Comparison of summer and winter inorganic carbon, oxygen and nutrient concentrations in Antarctic sea ice brine, Mar. Chem., 51, 81–91, https://doi.org/10.1016/0304-4203(95)00053-T, 1995.

Grotti, M., Soggia, F., Ianni, C., and Frache, R.: Trace metals distributions in coastal sea ice of Terra Nova Bay, Ross Sea, Antarctica, Antarct. Sci., 17, 289–300, https://doi.org/10.1017/S0954102005002695, 2005.

Günther, S. and Dieckmann, G. S.: Seasonal development of algal biomass in snow-covered fast ice and the underlying platelet layer in the Weddell Sea, Antarctica, Antarct. Sci., 11, 305–315, https://doi.org/10.1017/S0954102099000395, 1999.

Gutt, J., Starmans, A., and Dieckmann, G.: Impact of iceberg scouring on polar benthic habitats, Mar. Ecol. Prog. Ser., 137, 311–316, https://doi.org/10.3354/meps137311, 1996.

Halbach, L., Vihtakari, M., Duarte, P., Everett, A., Granskog, M. A., Hop, H., Kauko, H. M., Kristiansen, S., Myhre, P. I., Pavlov, A. K., Pramanik, A., Tatarek, A., Torsvik, T., Wiktor, J. M., Wold, A., Wulff, A., Steen, H., and Assmy, P.: Tidewater Glaciers and Bedrock Characteristics Control the Phytoplankton Growth Environment in a Fjord in the Arctic, Front. Mar. Sci., 31, https://doi.org/10.3389/fmars.2019.00254, 2019.

Hansen, H. P. and Koroleff, F.: Determination of nutrients, in: Methods of seawater analysis, edited by: Grasshoff, K., Kremling, K., and Ehrhardt, M., Wiley-VCH Verlag GmbH, 159–228, ISBN 9783527613984, 1999.

Hansson, M. E.: The Renland ice core. A Northern Hemisphere record of aerosol composition over 120 000 years, Tellus B, 46, 390–418, https://doi.org/10.1034/j.1600-0889.1994.t01-4-00005.x, 1994.

Hart, T. J.: Discovery Reports, Discovery Reports, VIII, 1–268, 1934.

Hawco, N. J., Tagliabue, A., and Twining, B. S.: Manganese Limitation of Phytoplankton Physiology and Productivity in the Southern Ocean, Global Biogeochem. Cy., 36, e2022GB007382, https://doi.org/10.1029/2022GB007382, 2022.

Hawkings, J. R., Wadham, J. L., Benning, L. G., Hendry, K. R., Tranter, M., Tedstone, A., Nienow, P., and Raiswell, R.: Ice sheets as a missing source of silica to the polar oceans, Nat. Commun., 8, 14198, https://doi.org/10.1038/ncomms14198, 2017.

Hawkings, J. R., Skidmore, M. L., Wadham, J. L., Priscu, J. C., Morton, P. L., Hatton, J. E., Gardner, C. B., Kohler, T. J., Stibal, M., Bagshaw, E. A., Steigmeyer, A., Barker, J., Dore, J. E., Lyons, W. B., Tranter, M., and Spencer, R. G. M.: Enhanced trace element mobilization by Earth's ice sheets, P. Natl. Acad. Sci. USA, 117, 31648–31659, https://doi.org/10.1073/pnas.2014378117, 2020.

Helly, J. J., Kaufmann, R. S., Stephenson Jr., G. R., and Vernet, M.: Cooling, dilution and mixing of ocean water by free-drifting icebergs in the Weddell Sea, Deep-Sea Res. Pt. II, 58, 1346–1363, https://doi.org/10.1016/j.dsr2.2010.11.010, 2011.

Henley, S. F., Cozzi, S., Fripiat, F., Lannuzel, D., Nomura, D., Thomas, D. N., Meiners, K. M., Vancoppenolle, M., Arrigo, K., Stefels, J., van Leeuwe, M., Moreau, S., Jones, E. M., Fransson, A., Chierici, M., and Delille, B.: Macronutrient biogeochemistry in Antarctic land-fast sea ice: Insights from a circumpolar data compilation, Mar. Chem., 257, 104324, https://doi.org/10.1016/j.marchem.2023.104324, 2023.

Herraiz-Borreguero, L., Lannuzel, D., van der Merwe, P., Treverrow, A., and Pedro, J. B.: Large flux of iron from the Amery Ice Shelf marine ice to Prydz Bay, East Antarctica, J. Geophys. Res.-Oceans, 121, 6009–6020, https://doi.org/10.1002/2016JC011687, 2016.

Höfer, J., González, H., Laudien, J., Schmidt, G., Häussermann, V., and Richter, C.: All you can eat: the functional response of the cold-water coral Desmophyllum dianthus feeding on krill and copepods, PeerJ, 6, e5872, https://doi.org/10.7717/peerj.5872, 2018.

Höfer, J., Giesecke, R., Hopwood, M. J., Carrera, V., Alarcón, E., and González, H. E.: The role of water column stability and wind mixing in the production/export dynamics of two bays in the Western Antarctic Peninsula, Prog. Oceanogr., 174, 105–116, https://doi.org/10.1016/j.pocean.2019.01.005, 2019.

Hopwood, M. J., Cantoni, C., Clarke, J. S., Cozzi, S., and Achterberg, E. P.: The heterogeneous nature of Fe delivery from melting icebergs, Geochem. Perspect. Lett., 3, 200–209, https://doi.org/10.7185/geochemlet.1723, 2017.

Hopwood, M. J., Carroll, D., Höfer, J., Achterberg, E. P., Meire, L., Le Moigne, F. A. C., Bach, L. T., Eich, C., Sutherland, D. A., and González, H. E.: Highly variable iron content modulates iceberg-ocean fertilisation and potential carbon export, Nat. Commun., 10, 5261, https://doi.org/10.1038/s41467-019-13231-0, 2019.

Hopwood, M. J., Carroll, D., Cozzi, S., Cantoni, C., and Körtzinger, A.: GLICE Freshwater biogeochemistry, EMODnet [data set], https://emodnet.ec.europa.eu/geonetwork/emodnet/api/records/ff3c625c-6a39-46ef-b329-222040f85917, 2023.

Huhn, O., Rhein, M., Kanzow, T., Schaffer, J., and Sültenfuß, J.: Submarine Meltwater From Nioghalvfjerdsbræ (79 North Glacier), Northeast Greenland, J. Geophys. Res.-Oceans, 126, e2021JC017224, https://doi.org/10.1029/2021JC017224, 2021.

IPCC: IPCC Special Report on the Ocean and Cryosphere in a Changing Climate, edited by: Pörtner, H.-O., Roberts, D. C., Masson-Delmotte, V., Zhai, P., Tignor, M., Poloczanska, E., Mintenbeck, K., Alegría, A., Nicolai, M., Okem, A., Petzold, J., Rama, B., and Weyer, N. M., Cambridge University Press, Cambridge, UK and New York, NY, USA, 755 pp. https://doi.org/10.1017/9781009157964, 2019.

Kandel, A. and Aguilar-Islas, A.: Spatial and temporal variability of dissolved aluminum and manganese in surface waters of the northern Gulf of Alaska, Deep-Sea Res. Pt. II, 189–190, 104952, https://doi.org/10.1016/j.dsr2.2021.104952, 2021.

Kim, J., Park, Y. K., Koo, T., Jung, J., Kang, I., Kim, K., Park, H., Yoo, K.-C., Rosenheim, B. E., and Conway, T. M.: Microbially-mediated reductive dissolution of Fe-bearing minerals during freeze-thaw cycles, Geochim. Cosmochim. Ac., 376, 134–143, https://doi.org/10.1016/j.gca.2024.05.015, 2024.

Kim, K., Choi, W., Hoffmann, M. R., Yoon, H.-I., and Park, B.-K.: Photoreductive Dissolution of Iron Oxides Trapped in Ice and Its Environmental Implications, Environ. Sci. Technol., 44, 4142–4148, https://doi.org/10.1021/es9037808, 2010.

Kjær, H. A., Dallmayr, R., Gabrieli, J., Goto-Azuma, K., Hirabayashi, M., Svensson, A., and Vallelonga, P.: Greenland ice cores constrain glacial atmospheric fluxes of phosphorus, J. Geophys. Res.-Atmos., 120, 10810–10822, https://doi.org/10.1002/2015JD023559, 2015.

Knight, P. G.: The basal ice layer of glaciers and ice sheets, Quaternary Sci. Rev., 16, 975–993, https://doi.org/10.1016/S0277-3791(97)00033-4, 1997.

Krause, J., Hopwood, M. J., Höfer, J., Krisch, S., Achterberg, E. P., Alarcón, E., Carroll, D., González, H. E., Juul-Pedersen, T., Liu, T., Lodeiro, P., Meire, L., and Rosing, M. T.: Trace Element (Fe, Co, Ni and Cu) Dynamics Across the Salinity Gradient in Arctic and Antarctic Glacier Fjords, Front. Earth Sci., 9, 878, https://doi.org/10.3389/feart.2021.725279, 2021.

Krause, J. W., Duarte, C. M., Marquez, I. A., Assmy, P., Fernández-Méndez, M., Wiedmann, I., Wassmann, P., Kristiansen, S., and Agustí, S.: Biogenic silica production and diatom dynamics in the Svalbard region during spring, Biogeosciences, 15, 6503–6517, https://doi.org/10.5194/bg-15-6503-2018, 2018.

Krause, J. W., Schulz, I. K., Rowe, K. A., Dobbins, W., Winding, M. H. S., Sejr, M. K., Duarte, C. M., and Agustí, S.: Silicic acid limitation drives bloom termination and potential car-

bon sequestration in an Arctic bloom, Sci. Rep.-UK, 9, 8149, https://doi.org/10.1038/s41598-019-44587-4, 2019.

Krisch, S., Browning, T. J., Graeve, M., Ludwichowski, K.-U., Lodeiro, P., Hopwood, M. J., Roig, S., Yong, J.-C., Kanzow, T., and Achterberg, E. P.: The influence of Arctic Fe and Atlantic fixed N on summertime primary production in Fram Strait, North Greenland Sea, Sci. Rep.-UK, 10, 15230, https://doi.org/10.1038/s41598-020-72100-9, 2020.

Latour, P., Wuttig, K., van der Merwe, P., Strzepek, R. F., Gault-Ringold, M., Townsend, A. T., Holmes, T. M., Corkill, M., and Bowie, A. R.: Manganese biogeochemistry in the Southern Ocean, from Tasmania to Antarctica, Limnol. Oceanogr., 66, 2547–2562, https://doi.org/10.1002/lno.11772, 2021.

Laufer-Meiser, K., Michaud, A. B., Maisch, M., Byrne, J. M., Kappler, A., Patterson, M. O., Røy, H., and Jørgensen, B. B.: Potentially bioavailable iron produced through benthic cycling in glaciated Arctic fjords of Svalbard, Nat. Commun., 12, 1349, https://doi.org/10.1038/s41467-021-21558-w, 2021.

Lewis, E. L. and Perkin, R. G.: Ice pumps and their rates, J. Geophys. Res.-Oceans, 91, 11756–11762, https://doi.org/10.1029/JC091iC10p11756, 1986.

Lin, H. and Twining, B. S.: Chemical speciation of iron in Antarctic waters surrounding free-drifting icebergs, Mar. Chem., 128, 81–91, https://doi.org/10.1016/j.marchem.2011.10.005, 2012.

Lin, H., Rauschenberg, S., Hexel, C. R., Shaw, T. J., and Twining, B. S.: Free-drifting icebergs as sources of iron to the Weddell Sea, Deep-Sea Res. Pt. II, 58, 1392–1406, https://doi.org/10.1016/j.dsr2.2010.11.020, 2011.

Lippiatt, S. M., Lohan, M. C., and Bruland, K. W.: The distribution of reactive iron in northern Gulf of Alaska coastal waters, Mar. Chem., 121, 187–199, https://doi.org/10.1016/j.marchem.2010.04.007, 2010.

Loscher, B. M., DeBaar, H. J. W., DeJong, J. T. M., Veth, C., and Dehairs, F.: The distribution of Fe in the Antarctic Circumpolar Current, Deep-Sea Res. Pt. II, 44, 143–187, https://doi.org/10.1016/S0967-0645(96)00101-4, 1997.

Martin, J. H., Fitzwater, S. E., and Gordon, R. M.: Iron deficiency limits phytoplankton growth in Antarctic waters, Global Biogeochem. Cy., 4, 5–12, https://doi.org/10.1029/GB004i001p00005, 1990a.

Martin, J. H., Gordon, R. M., and Fitzwater, S. E.: Iron in Antarctic waters, Nature, 345, 156–158, https://doi.org/10.1038/345156a0, 1990b.

Meire, L., Meire, P., Struyf, E., Krawczyk, D. W., Arendt, K. E., Yde, J. C., Juul Pedersen, T., Hopwood, M. J., Rysgaard, S., and Meysman, F. J. R.: High export of dissolved silica from the Greenland Ice Sheet, Geophys. Res. Lett., 43, 9173–9182, https://doi.org/10.1002/2016GL070191, 2016.

Meire, L., Mortensen, J., Meire, P., Juul-Pedersen, T., Sejr, M. K., Rysgaard, S., Nygaard, R., Huybrechts, P., and Meysman, F. J. R.: Marine-terminating glaciers sustain high productivity in Greenland fjords, Global Change Biol., 23, 5344–5357, https://doi.org/10.1111/gcb.13801, 2017.

Moon, T., Sutherland, D. A., Carroll, D., Felikson, D., Kehrl, L., and Straneo, F.: Subsurface iceberg melt key to Greenland fjord freshwater budget, Nat. Geosci., 11, 49–54, https://doi.org/10.1038/s41561-017-0018-z, 2018.

Moore, C. M., Mills, M. M., Arrigo, K. R., Berman-Frank, I., Bopp, L., Boyd, P. W., Galbraith, E. D., Geider, R. J., Guieu, C., Jaccard, S. L., Jickells, T. D., La Roche, J., Lenton, T. M., Mahowald, N. M., Maranon, E., Marinov, I., Moore, J. K., Nakatsuka, T., Oschlies, A., Saito, M. A., Thingstad, T. F., Tsuda, A., and Ulloa, O.: Processes and patterns of oceanic nutrient limitation, Nat. Geosci., 6, 701–710, https://doi.org/10.1038/ngeo1765, 2013.

Mugford, R. I. and Dowdeswell, J. A.: Modeling iceberg-rafted sedimentation in high-latitude fjord environments, J. Geophys. Res.-Earth, 115, F03024, https://doi.org/10.1029/2009JF001564, 2010.

Neubauer, J. and Heumann, K. G.: Nitrate trace determinations in snow and firn core samples of ice shelves at the weddell sea, Antarctica, Atmos. Environ., 22, 537–545, https://doi.org/10.1016/0004-6981(88)90197-7, 1988.

Nielsdottir, M. C., Moore, C. M., Sanders, R., Hinz, D. J., and Achterberg, E. P.: Iron limitation of the postbloom phytoplankton communities in the Iceland Basin, Global Biogeochem. Cy., 23, GB3001, https://doi.org/10.1029/2008gb003410, 2009.

Nomura, D., Sahashi, R., Takahashi, K. D., Makabe, R., Ito, M., Tozawa, M., Wongpan, P., Matsuda, R., Sano, M., Yamamoto-Kawai, M., Nojiro, N., Tachibana, A., Kurosawa, N., Moteki, M., Tamura, T., Aoki, S., and Murase, H.: Biogeochemical characteristics of brash sea ice and icebergs during summer and autumn in the Indian sector of the Southern Ocean, Prog. Oceanogr., 214, 103023, https://doi.org/10.1016/j.pocean.2023.103023, 2023.

Oerter, H., Kipfstuhl, J., Determann, J., Miller, H., Wagenbach, D., Minikin, A., and Graft, W.: Evidence for basal marine ice in the Filchner–Ronne ice shelf, Nature, 358, 399–401, https://doi.org/10.1038/358399a0, 1992.

Oksanen, J., Blanchet, F. G., Friendly, M., Kindt, R., Legendre, P., McGlinn, D., Minchin, P. R., O'Hara, R. B., Simpson, G. L., Solymos, P., H., Stevens, M. H. H., Szoecs, E., and Wagner, H.: vegan: Community Ecology Package version 2.5-7, https://github.com/vegandevs/vegan (last acces: November 2024), 2020.

Parker, B. C., Heiskell, L. E., Thompson, W., and Zeller, E. J.: Non-biogenic fixed nitrogen in Antarctica and some ecological implications, Nature, 271, 651–652, https://doi.org/10.1038/271651a0, 1978.

Peñuelas, J., Sardans, J., Rivas-ubach, A., and Janssens, I. A.: The human-induced imbalance between C, N and P in Earth's life system, Global Change Biol., 18, 3–6, https://doi.org/10.1111/j.1365-2486.2011.02568.x, 2012.

Person, R., Vancoppenolle, M., Aumont, O., and Malsang, M.: Continental and Sea Ice Iron Sources Fertilize the Southern Ocean in Synergy, Geophys. Res. Lett., 48, e2021GL094761, https://doi.org/10.1029/2021GL094761, 2021.

R Core Team: R: A Language and Environment for Statistical Computing, https://www.R-project.org/ (last acces: November 2024), 2023.

Raiswell, R.: Iceberg-hosted nanoparticulate Fe in the Southern Ocean: Mineralogy, origin, dissolution kinetics and source of bioavailable Fe, Deep-Sea Res. Pt. II, 58, 1364–1375, https://doi.org/10.1016/j.dsr2.2010.11.011, 2011.

Raiswell, R., Benning, L. G., Tranter, M., and Tulaczyk, S.: Bioavailable iron in the Southern Ocean: the significance of the iceberg conveyor belt, Geochem. T., 9, 7, https://doi.org/10.1186/1467-4866-9-7, 2008.

Randelhoff, A., Holding, J., Janout, M., Sejr, M. K., Babin, M., Tremblay, J. É., and Alkire, M. B.: Pan-Arctic Ocean Primary

Production Constrained by Turbulent Nitrate Fluxes, Front. Mar. Sci., 7, https://doi.org/10.3389/fmars.2020.00150, 2020.

Redfield, A. C.: On the proportions of organic derivations in sea water and their relation to the composition of plankton, in: James Johnstone Memorial Volume, edited by: Daniel, R. J., University Press of Liverpool, Liverpool, 177–192, 1934.

Rignot, E., Jacobs, S., Mouginot, J., and Scheuchl, B.: Ice-Shelf Melting Around Antarctica, Science, 341, 266–270, https://doi.org/10.1126/science.1235798, 2013.

Rozwalak, P., Podkowa, P., Buda, J., Niedzielski, P., Kawecki, S., Ambrosini, R., Azzoni, R. S., Baccolo, G., Ceballos, J. L., Cook, J., Di Mauro, B., Ficetola, G. F., Franzetti, A., Ignatiuk, D., Klimaszyk, P., Łokas, E., Ono, M., Parnikoza, I., Pietryka, M., Pittino, F., Poniecka, E., Porazinska, D. L., Richter, D., Schmidt, S. K., Sommers, P., Souza-Kasprzyk, J., Stibal, M., Szczuciński, W., Uetake, J., Wejnerowski, Ł., Yde, J. C., Takeuchi, N., and Zawierucha, K.: Cryoconite – From minerals and organic matter to bioengineered sediments on glacier's surfaces, Sci. Total Environ., 807, 150874, https://doi.org/10.1016/j.scitotenv.2021.150874, 2022.

Rudnick, R. L. and Gao, S.: Composition of the continental crust, in: Treatise on geochemistry, vol. 3, The Crust, edited by: Holland, H. D. and Turekian, K. K., Elsevier, Amsterdam, 1–65, https://doi.org/10.1016/B0-08-043751-6/03016-4, 2003.

Ryan-Keogh, T. J., Macey, A. I., Nielsdottir, M. C., Lucas, M. I., Steigenberger, S. S., Stinchcombe, M. C., Achterberg, E. P., Bibby, T. S., and Moore, C. M.: Spatial and temporal development of phytoplankton iron stress in relation to bloom dynamics in the high-latitude North Atlantic Ocean, Limnol. Oceanogr., 58, 533–545, https://doi.org/10.4319/lo.2013.58.2.0533, 2013.

Schwarz, J. N. and Schodlok, M. P.: Impact of drifting icebergs on surface phytoplankton biomass in the Southern Ocean: Ocean colour remote sensing and in situ iceberg tracking, Deep-Sea Res. Pt. I, 56, 1727–1741, https://doi.org/10.1016/j.dsr.2009.05.003, 2009.

Sedwick, P. N., DiTullio, G. R., and Mackey, D. J.: Iron and manganese in the Ross Sea, Antarctica: Seasonal iron limitation in Antarctic shelf waters, J. Geophys. Res.-Oceans, 105, 11321–11336, https://doi.org/10.1029/2000jc000256, 2000.

Shaw, T. J., Raiswell, R., Hexel, C. R., Vu, H. P., Moore, W. S., Dudgeon, R., and Smith Jr., K. L.: Input, composition, and potential impact of terrigenous material from free-drifting icebergs in the Weddell Sea, Deep-Sea Res. Pt. II, 58, 1376–1383, https://doi.org/10.1016/j.dsr2.2010.11.012, 2011.

Shulenberger, E.: Water-column studies near a melting Arctic iceberg, Polar Biol., 2, 149–158, https://doi.org/10.1007/BF00448964, 1983.

Smith Jr., K. L., Robison, B. H., Helly, J. J., Kaufmann, R. S., Ruhl, H. A., Shaw, T. J., Twining, B. S., and Vernet, M.: Free-drifting icebergs: Hot spots of chemical and biological enrichment in the Weddell Sea, Science, 317, 478–482, https://doi.org/10.1126/science.1142834, 2007.

Smith, J. A., Graham, A. G. C., Post, A. L., Hillenbrand, C.-D., Bart, P. J., and Powell, R. D.: The marine geological imprint of Antarctic ice shelves, Nat. Commun., 10, 5635, https://doi.org/10.1038/s41467-019-13496-5, 2019.

Stephenson, G. R., Sprintall, J., Gille, S. T., Vernet, M., Helly, J. J., and Kaufmann, R. S.: Subsurface melting of a free-floating Antarctic iceberg, Deep-Sea Res. Pt. II, 58, 1336–1345, https://doi.org/10.1016/j.dsr2.2010.11.009, 2011.

Stibal, M., Box, J. E., Cameron, K. A., Langen, P. L., Yallop, M. L., Mottram, R. H., Khan, A. L., Molotch, N. P., Chrismas, N. A. M., Calì Quaglia, F., Remias, D., Smeets, C. J. P. P., van den Broeke, M. R., Ryan, J. C., Hubbard, A., Tranter, M., van As, D., and Ahlstrøm, A. P.: Algae Drive Enhanced Darkening of Bare Ice on the Greenland Ice Sheet, Geophys. Res. Lett., 44, 11463–11471, https://doi.org/10.1002/2017GL075958, 2017.

Sunda, W. G. and Huntsman, S. A.: Effect of sunlight on redox cycles of manganese in the southwestern Sargasso Sea, Deep-Sea Res., 35, 1297–1317, https://doi.org/10.1016/0198-0149(88)90084-2, 1988.

Sunda, W. G., Huntsman, S. A., and Harvey, G. R.: Photoreduction of manganese oxides in seawater and its geochemical and biological implications, Nature, 301, 234–236, https://doi.org/10.1038/301234a0, 1983.

Syvitski, J. P. M., Burrell, D. C., and Skei, J. M.: Fjords, Springer New York, https://doi.org/10.1007/978-1-4612-4632-9, 1987.

Tarling, G. A., Thorpe, S. E., Henley, S. F., Burson, A., Liszka, C. M., Manno, C., Lucas, N. S., Ward, F., Hendry, K. R., Malcolm S. Woodward, E., Wootton, M., and Povl Abrahamsen, E.: Collapse of a giant iceberg in a dynamic Southern Ocean marine ecosystem: In situ observations of A-68A at South Georgia, Prog. Oceanogr., 226, 103297, https://doi.org/10.1016/j.pocean.2024.103297, 2024.

Tournadre, J., Bouhier, N., Girard-Ardhuin, F., and Rémy, F.: Antarctic icebergs distributions 1992–2014, J. Geophys. Res.-Oceans, 121, 327–349, https://doi.org/10.1002/2015JC011178, 2016.

Tranter, M., Skidmore, M., and Wadham, J.: Hydrological controls on microbial communities in subglacial environments, Hydrol. Process., 19, 995–998, https://doi.org/10.1002/hyp.5854, 2005.

Trefault, N., De la Iglesia, R., Moreno-Pino, M., Lopes dos Santos, A., Gérikas Ribeiro, C., Parada-Pozo, G., Cristi, A., Marie, D., and Vaulot, D.: Annual phytoplankton dynamics in coastal waters from Fildes Bay, Western Antarctic Peninsula, Sci. Rep.-UK, 11, 1368, https://doi.org/10.1038/s41598-020-80568-8, 2021.

Vancoppenolle, M., Goosse, H., de Montety, A., Fichefet, T., Tremblay, B., and Tison, J.-L.: Modeling brine and nutrient dynamics in Antarctic sea ice: The case of dissolved silica, J. Geophys. Res.-Oceans, 115, C02005, https://doi.org/10.1029/2009JC005369, 2010.

van Genuchten, C. M., Hopwood, M. J., Liu, T., Krause, J., Achterberg, E. P., Rosing, M. T., and Meire, L.: Solid-phase Mn speciation in suspended particles along meltwater-influenced fjords of West Greenland, Geochim. Cosmochim. Ac., 326, 180–198, https://doi.org/10.1016/j.gca.2022.04.003, 2022.

Vernet, M., Sines, K., Chakos, D., Cefarelli, A. O., and Ekern, L.: Impacts on phytoplankton dynamics by free-drifting icebergs in the NW Weddell Sea, Deep-Sea Res. Pt. II, 58, 1422–1435, https://doi.org/10.1016/j.dsr2.2010.11.022, 2011.

Wadham, J. L., Tranter, M., Skidmore, M., Hodson, A. J., Priscu, J., Lyons, W. B., Sharp, M., Wynn, P., and Jackson, M.: Biogeochemical weathering under ice: Size matters, Global Biogeochem. Cy., 24, GB3025, https://doi.org/10.1029/2009gb003688, 2010.

Wehrmann, L. M., Formolo, M. J., Owens, J. D., Raiswell, R., Ferdelman, T. G., Riedinger, N., and Lyons, T. W.:

Iron and manganese speciation and cycling in glacially influenced high-latitude fjord sediments (West Spitsbergen, Svalbard): Evidence for a benthic recycling-transport mechanism, Geochim. Cosmochim. Ac., 141, 628–655, https://doi.org/10.1016/j.gca.2014.06.007, 2013.

Woodworth-Lynas, C. M. T., Josenhans, H. W., Barrie, J. V, Lewis, C. F. M., and Parrott, D. R.: The physical processes of seabed disturbance during iceberg grounding and scouring, Cont. Shelf Res., 11, 939–961, https://doi.org/10.1016/0278-4343(91)90086-L, 1991.

Wu, M., McCain, J. S. P., Rowland, E., Middag, R., Sandgren, M., Allen, A. E., and Bertrand, E. M.: Manganese and iron deficiency in Southern Ocean Phaeocystis antarctica populations revealed through taxon-specific protein indicators, Nat. Commun., 10, 3582, https://doi.org/10.1038/s41467-019-11426-z, 2019.

Wu, S.-Y. and Hou, S.: Impact of icebergs on net primary productivity in the Southern Ocean, The Cryosphere, 11, 707–722, https://doi.org/10.5194/tc-11-707-2017, 2017.

Yang, Y., Ren, J., and Zhu, Z.: Distributions and Influencing Factors of Dissolved Manganese in Kongsfjorden and Ny-Ålesund, Svalbard, ACS Earth Space Chem, 6, 1259–1268, https://doi.org/10.1021/acsearthspacechem.1c00388, 2022.

Zhang, R., John, S. G., Zhang, J., Ren, J., Wu, Y., Zhu, Z., Liu, S., Zhu, X., Marsay, C. M., and Wenger, F.: Transport and reaction of iron and iron stable isotopes in glacial meltwaters on Svalbard near Kongsfjorden: From rivers to estuary to ocean, Earth Planet. Sc. Lett., 424, 201–211, https://doi.org/10.1016/j.epsl.2015.05.031, 2015.